ENVIRONMENTAL RESEARCH
LETTERS

LETTER • OPEN ACCESS

The social cost of carbon dioxide under climate-economy feedbacks and temperature variability

IOP Publishing Environ. Res. Lett. 16 (2021) 094037 https://doi.org/10.1088/1748-9326/ac1d0b

ENVIRONMENTAL RESEARCH
LETTERS

OPEN ACCESS

RECEIVED
27 March 2021

REVISED
20 July 2021

ACCEPTED FOR PUBLICATION
12 August 2021

PUBLISHED
6 September 2021

LETTER

The social cost of carbon dioxide under climate-economy feedbacks and temperature variability

Jarmo S Kikstra[1,2,3,4,*], **Paul Waidelich**[5,6], **James Rising**[5], **Dmitry Yumashev**[7,8], **Chris Hope**[9] and **Chris M Brierley**[2]

[1] International Institute for Applied Systems Analysis (IIASA), Laxenburg, Austria
[2] Department of Geography, University College London, London, United Kingdom
[3] Centre for Environmental Policy, Imperial College London, London, United Kingdom
[4] Grantham Institute for Climate Change and the Environment, Imperial College London, London, United Kingdom
[5] Grantham Research Institute on Climate Change and the Environment, London School of Economics, London, United Kingdom
[6] NERA Economic Consulting, Berlin, Germany
[7] Lancaster University, Pentland Centre for Sustainability in Business, Lancaster, United Kingdom
[8] Institute of Sustainable Resources, University College London, London, United Kingdom
[9] Judge Business School, University of Cambridge, Cambridge, United Kingdom
[*] Author to whom any correspondence should be addressed.

E-mail: kikstra@iiasa.ac.at

Keywords: climate change, cost–benefit analysis, temperature variability, damage persistence, growth effects, PAGE, environmental economics

Abstract

A key statistic describing climate change impacts is the 'social cost of carbon dioxide' ($SCCO_2$), the projected cost to society of releasing an additional tonne of CO_2. Cost-benefit integrated assessment models that estimate the $SCCO_2$ lack robust representations of climate feedbacks, economy feedbacks, and climate extremes. We compare the PAGE-ICE model with the decade older PAGE09 and find that PAGE-ICE yields $SCCO_2$ values about two times higher, because of its climate and economic updates. Climate feedbacks only account for a relatively minor increase compared to other updates. Extending PAGE-ICE with economy feedbacks demonstrates a manifold increase in the $SCCO_2$ resulting from an empirically derived estimate of partially persistent economic damages. Both the economy feedbacks and other increases since PAGE09 are almost entirely due to higher damages in the Global South. Including an estimate of interannual temperature variability increases the width of the $SCCO_2$ distribution, with particularly strong effects in the tails and a slight increase in the mean $SCCO_2$. Our results highlight the large impacts of climate change if future adaptation does not exceed historical trends. Robust quantification of climate-economy feedbacks and climate extremes are demonstrated to be essential for estimating the $SCCO_2$ and its uncertainty.

1. Introduction

One crucial indicator of the level of urgency for taking climate action is the social cost of carbon dioxide ($SCCO_2$), which represents the total welfare lost across the globe due to an extra emitted tonne of CO_2, usually expressed in US dollars per tonne of CO_2. The $SCCO_2$ has been calculated under a range of climatic and socioeconomic assumptions (Havranek *et al* 2015, Howard and Sterner 2017, Tol 2018), giving a wide range of best estimates. These contemporary estimates are often higher than values that have been used in policies or the economy-wide average price on CO_2 emissions (Dolphin *et al* 2020), in part due to underestimates of impacts and strong discounting assumptions of future damages in policy-making (Carleton and Greenstone 2021, Wagner *et al* 2021). Current policy recommendations range from US$51 (Interagency Working Group 2013) to US$202 (Umwelt Bundesamt 2019), while a recent expert elicitation among economists and climate scientists yielded mean values of US$171 and US$310, respectively (Pindyck 2019). Other central estimates are even higher (Moore and Diaz 2015, Ricke *et al* 2018). Many challenges remain to improve estimates of the $SCCO_2$ estimates as well as the related

uncertainty range (National Academies of Sciences Engineering and Medicine 2017, Stern and Stiglitz 2021, Wagner *et al* 2021), which is of critical value for designing comprehensive climate mitigation and adaptation policies (Smith and Stern 2011, Hope 2015, Metcalf and Stock 2017).

Cost-benefit integrated assessment models (CB-IAMs) representing climate-economy interactions in a highly aggregated manner and have been key tools to estimating the $SCCO_2$. Unfortunately, these models lag behind both natural and social science understanding, often undervaluing the impacts of climate change (Diaz and Moore 2017, Howard and Sterner 2017, Rose *et al* 2017, Carleton and Greenstone 2021). In particular, CB-IAMs have only simple representations of climate and economy feedbacks, which are key determinants of climate change risks (Otto *et al* 2013, Calvin *et al* 2019). Many authors thus argue that rigorous inclusion of the feedbacks is crucial in calculating the $SCCO_2$ (Burke *et al* 2016, Cai *et al* 2016, National Academies of Sciences Engineering and Medicine 2017, Stiglitz *et al* 2017, Piontek *et al* 2021).

As for climate feedbacks, previous research has calculated the mean discounted economic effect of climate change with selected state-dependent climate feedbacks, but provided no breakdown of regional or distributional implications of marginal damages of CO_2 emissions (Cai *et al* 2016, Yumashev *et al* 2019). Here, we compare the PAGE-ICE CB-IAM which also introduced permafrost thawing and surface albedo climate feedbacks (Yumashev *et al* 2019) with PAGE09 (Hope 2013) and attribute the changes in the $SCCO_2$ to the specific model changes.

How temperature rises affect long-run economic output is an important open question (Piontek *et al* 2021). Climate impacts could either trigger additional GDP growth due to increased agricultural productivity and rebuilding activities (Stern 2007, Hallegatte and Dumas 2009, Hsiang 2010, National Academies of Sciences Engineering and Medicine 2017) or inhibit growth due to damaged capital stocks (Pindyck 2013), lower savings (Fankhauser and Tol 2005) and inefficient factor reallocation (Piontek *et al* 2019). Existing studies have identified substantial impacts of economic growth feedbacks (Moyer *et al* 2014, Dietz and Stern 2015, Estrada *et al* 2015, Moore and Diaz 2015), but have not yet quantified the uncertainties involved based on empirical distributions. One particular example is Kalkuhl and Wenz (2020), who incorporate short-term economic persistence into a recent version of DICE (Nordhaus 2017), approximately tripling the resulting $SCCO_2$ ($37–$132). For fairly comparable economic assumptions, the effect of long-term persistence is shown to increase the outcome even more ($220–$417) (Moore and Diaz 2015, Ricke *et al* 2018). We further expand on this work by deriving an empirical distribution of the persistence of climate impacts on economic growth based on recent developments (Burke *et al* 2015, Bastien-Olvera and Moore 2021) which we use to moderate GDP growth through persistent market damages. This partial persistence model builds upon recent empirical insights that not all contemporary economic damages due to climate change might be recovered in the long run (Dell *et al* 2012, Burke *et al* 2015, Kahn *et al* 2019, Bastien-Olvera and Moore 2021). Investigating how the $SCCO_2$ varies as a function of the extent of persistence reveals a sensitivity that is on par with the heavily discussed role of discounting (Anthoff *et al* 2009b).

Climatic extremes are another particularly important driver of climate change-induced damages (Field *et al* 2012, Kotz *et al* 2021). The impact of interannual climate variability on the $SCCO_2$ has, however, not been analyzed previously, despite its clear economic implications (Burke *et al* 2015, Kahn *et al* 2019, Kumar and Khanna 2019) and an apparent relation to weather extremes such as daily minima and maxima (Seneviratne *et al* 2012), extreme rainfall (Jones *et al* 2013), and floods (Marsh *et al* 2016). Omission of such features in climate-economy models risks underestimation of the $SCCO_2$ because if convex regional temperature damage functions (Burke *et al* 2015) and an expected earlier crossing of potential climate and social thresholds in the climate-economy system (Tol 2019, Glanemann *et al* 2020). Here, we include climate variability by coupling the empirical temperature-damage function with variable, autoregressive interannual temperatures. Increasing the amount of uncertainty by adding variable elements naturally leads to a less constrained estimate for climate-driven impacts. However, it is important to explore the range of possible futures, including the consideration of extremes in the climate-economy system (Otto *et al* 2020).

In summary, we extend the PAGE-ICE CB-IAM (Yumashev *et al* 2019) to quantify the effect on the $SCCO_2$ of including possible long-term temperature growth feedback on economic trajectories, mean annual temperature anomalies, and the already modeled permafrost carbon and surface albedo feedbacks. Together, these provide an indication of the magnitude and uncertainties of the contribution of climate and economy feedbacks and interannual variability to the $SCCO_2$.

2. Methods

The PAGE-ICE model (Yumashev *et al* 2019) simulates climatic and economic developments between 2020 and 2300 in eight aggregated regions (appendix A.1) and extends PAGE09, building on a decade of scientific progress through improved representations of climatic processes and economic damages (figure 1). In particular, PAGE-ICE implements detailed models of Arctic feedbacks, consisting of permafrost thawing, and sea ice and land snow albedo

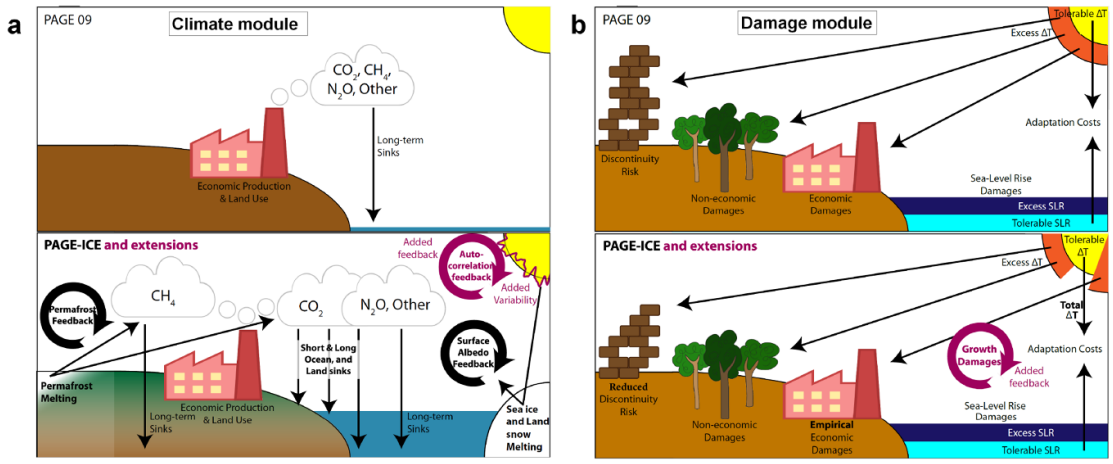

Figure 1. Illustrative sketch of changes and extensions to PAGE-ICE presented in this paper. (a) Changes in the climate representation. PAGE-ICE includes a more detailed representation of CO_2 and CH_4 sinks, permafrost carbon feedback, the effect of sea ice and land snow decline on surface albedo, and a fat-tailed distribution of sea level rise. Here we also include interannual temperature variability with a temperature feedback through annual auto-correlation. (b) Changes in the damage module. The PAGE-ICE discontinuity damage component was reduced to correspond with updates to climate tipping points and sea-level rise risk, and market damages were recalibrated to an empirical estimate based on temperatures. Thus, while the discontinuity and non-economic damages continue to be calculated based on the separation between tolerable and excess temperature, the market damages are now calculated based on absolute temperature. Here we also extend PAGE-ICE with the possibility of persistent climate-induced damages, which in turn affects GDP pathways and scales emissions accordingly (feedback loop in the figure).

changes. It also updates the climate representation to conform to parameters in the IPCC AR5 (Stocker *et al* 2013), and offers a wide range of consistent combined emissions and socioeconomic pathways. PAGE-ICE models temperature responses and greenhouse gas cycles including feedbacks for six emissions classes (CO_2, CH_4, N_2O, linear gases, sulphates, and a residual group for other greenhouse gas emissions). Global temperatures are scaled to the eight represented regions, before considering economic impacts (more detail in model documentation and supplementary information of Yumashev *et al* 2019). Economic damages due to rising temperatures are calibrated based on historic data and capture the heterogeneous response of countries to warming (Burke *et al* 2015), but the original PAGE-ICE does not simulate damage persistence. Thus, the economy always returns to the exogenous economic growth path, no matter how high the contemporary damages.

2.1. Model setup

Our setup recognizes that deterministic assessments of the $SCCO_2$ carry only very limited information. PAGE-ICE uses Monte Carlo sampling of over 150 parameter distributions (Yumashev *et al* 2019) to provide distributions of the results. All results presented use 50 000 Monte Carlo draws (and 100 000 for PAGE09, using @RISK within Excel), with draws taken from the same superset to be able to compare $SCCO_2$ distributions across models. The PAGE-ICE model has been translated into the Mimi modeling framework, using the same validation process as for Mimi-PAGE (Moore *et al* 2018). Model code and documentation are available from the GitHub repository, https://github.com/openmodels/MimiPAGE2020.jl.

To estimate the marginal damage of an additional tonne of CO_2, PAGE-ICE is run twice, with one run following the exogenously specified emission pathway and the second run adding a CO_2 pulse. The $SCCO_2$ is then calculated as the difference in global equity-weighted damages between those two runs divided by the pulse size, discounted to the base year (2015). Equity weighting of damages follows the approach by Anthoff *et al* (2009a) using a mean (minimum, maximum) elasticity of marginal utility of consumption of 1.17 (0.1–2.0), and equity-weighted damages are discounted using a pure time preference rate of 1.03% (0.5%, 2.0%). For all our results, we rely on a 75Gt pulse size in the first time period of PAGE-ICE (mid-2017–2025), representing an annual pulse size of 10 Gt CO_2. In this setup, we found that the choice of pulse size can have an effect on the $SCCO_2$ estimates, and we explore these sensitivities in appendix A.2, alongside a general sensitivity analysis of PAGE-ICE's model parameters in appendix A.3.

2.2. Scenarios

We provide results for a selection of scenarios across climate outcomes and socioeconomic developments, based on the Tier 1 scenarios of ScenarioMIP (O'Neill *et al* 2016). SSP1-1.9 and SSP1-2.6 are generally well aligned with the Paris Agreement (IPCC 2018, Rogelj *et al* 2018), while SSP5-8.5 features very high radiative forcing and rapid GDP growth. The 'middle-of-the-road' socioeconomic pathway SSP2 is combined with the emission pathway RCP4.5 scenario for the central values presented in this analysis. Since reference SSP scenarios are provided until 2100, we extend these by

making the assumption that regional GDP per capita and population growth rates in the different model regions converge toward the global mean. We implement this by defining a region's post-2100 growth rate as $g_{r,t} = (1 - DR - CR) \cdot g_{r,t-1} + CR \cdot \bar{g}_{t-1}$, where CR and DR are the respective universal rates of convergence and decay, and $\bar{g}$ is the global mean growth rate. The subscripts r, t represent region and time period, respectively. We fit the convergence and decay rates based on SSP growth rates up to 2100 using Stan, a Bayesian MCMC system (appendix A.5).

2.3. Persistence of damages

We implement the persistence parameter following Estrada *et al* (2015) into the growth system of Burke *et al* (2015) such that: $\mathrm{GDP}_{r,t} = \mathrm{GDP}_{r,t-1} \cdot (1 + g_{r,t} - \rho \cdot \gamma_{r,t-1})$, where g is the growth rate, γ represents the contemporary economic damages in % of GDP returned by the market damage function and ρ specifies the share of economic damages that persist and thus alter the growth trajectory in the long run. Note that this approach nests the extreme assumptions of zero persistence usually made in CB-IAMs and the assumption of full persistence from the empirical literature (Burke *et al* 2015, Ricke *et al* 2018) for $\rho = 0$ and $\rho = 1$, respectively. For consistency with the underlying RCP-SSP scenarios, we also rescale greenhouse gas emissions proportionally to the change in GDP, such that emission intensities of economic output remain unchanged. To estimate the distribution of ρ, we calculate the ratio of the long-run marginal impact of temperature on economic growth to the immediate marginal impact using the historical panel data by Burke *et al* (2015) (appendix B.3). For estimating the long-run marginal impact, we follow the literature in estimating regression models featuring temperature lags (Dell *et al* 2012, Burke *et al* 2015), and we additionally apply a more recent approach using low-pass filtering by Bastien-Olvera and Moore (2021) for robustness checks (appendix B.4).

For our aggregated analysis, we do not include any sectoral distinction for the persistence parameter ρ since PAGE-ICE models economic damages on the aggregated macro level using the damage function by Burke *et al* (2015). By taking one global value distribution for the ρ parameter, we assume that the persistence of damages is similar in each region modeled. Reduced significance for non-global estimates of partial persistence hinders the use of region-specific parameters. For all central results, damage persistence also remains constant over time following from the limited evidence for successful adaptation to date (Burke *et al* 2015, Burke and Emerick 2016). We explore these simplifications in detail in appendix B.5, where we consider a case that sees economically persistent damages only in lower-income regions, following suggestive evidence for regional heterogeneity, for instance due to higher climate vulnerability and reduced adaptive capacity (Byers *et al* 2018, Andrijevic *et al* 2020). Furthermore, we discuss the impacts of possible future adaptation reducing the persistence of temperature impacts on GDP (see also appendix B.6).

2.4. PAGE with annual temperature variability

To allow for modeling annual temperature anomalies, the inputs to the temperature and GDP modules of PAGE are annualized by a combination of exponential interpolation for population, sea-level rise, and abatement costs, and linear interpolation for GDP growth rates. Annualized temperatures are subsequently used for calculating the damages on an annual basis for the non-market, market, and discontinuity modules. Sea-level rise and consequent damages are modelled to depend on the global climatic mean temperatures modeled in PAGE-ICE, rather than annual on mean temperatures.

There is no strong evidence for the increase or decrease in global annual temperature variability with global mean temperature increases (Huntingford *et al* 2013, Sippel *et al* 2015). Therefore, we model the magnitude of interannual temperature variability to be constant over time, based on the analysis of regional means in a recent spatially complete dataset (Ilyas *et al* 2017) that is suitable for the analysis of temperature variability because its underlying statistical simulation approach allows for a more adequate approximation of the expected local variability and its uncertainty (Beguería *et al* 2016). We model global (1*a*) and regional (1*b*) temperature variability as follows:

$$T_{g,t+1} \sim \mathcal{N}(\alpha_g + \beta_g \Theta_{gt} + \gamma_g T_t, \sigma_g^2) \qquad (1a)$$

$$T_{r,t+1} \sim \mathcal{N}(\alpha_r + \beta_r T_{rt} + \gamma_g T_{g,t+1}, \sigma_r^2) \qquad (1b)$$

here, T is the realized annual temperature, Θ is the mean temperature realized in the PAGE climate module prior to variability, σ is the standard deviation of internal variability, and the subscripts g, r, t represent *global*, *regional*, and *time* (in years). In the absence of auto-regressive feedback, $\alpha_g = \alpha_r = \gamma_g = \gamma_r = 0$, $\beta_g = 1$, and $\beta_r = AF_r$, the regional amplification factor from PAGE-ICE. The temporal standard deviations σ are derived from annual spatially aggregated regional mean temperatures. These regional temperatures are derived from median gridded observations of 10 000 statistical ensemble members (Ilyas *et al* 2017), which are area-weighted and linearly detrended for a 30 year climatic period. Further information including uncertainties in these observations are found in appendix C.1. With autoregression, we fit all parameters to historical temperatures using least-squares regression, and applying a LOESS of global temperatures as Θ_{gt} (appendix C.2). As a robustness check, we include a simple alternative implementation of variability (appendix C.3).

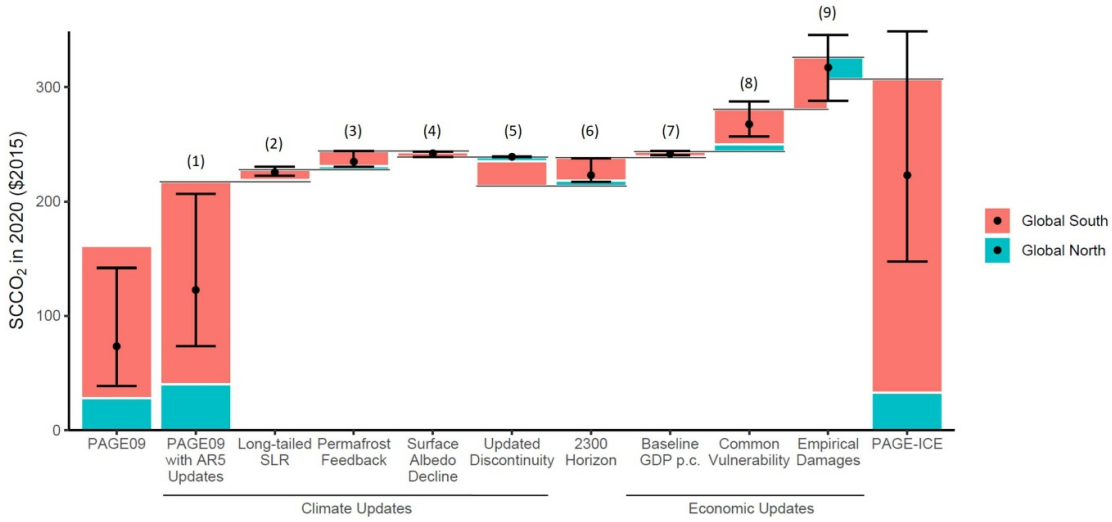

Figure 2. Estimates of the $SCCO_2$ for the model updates from PAGE09 to PAGE-ICE. Bars show the mean $SCCO_2$ or the mean difference across Monte Carlo runs. Mean differences are calculated for each draw of the Monte Carlo, so that uncertain parameters are consistent wherever possible. Error bars show the interquartile range with the median shown as a point. Description of the changes provided in the text. The 'AR5 Updates' bar is not represented as a difference, since these are calculated across modifications of PAGE-ICE, and the AR5 Updates bar represents the nearest equivalent to PAGE09. Note that due to interaction effects, changing the order in which changes are introduced can lead to minor changes in the values presented here.

3. Results

3.1. Climate feedbacks and $SCCO_2$ changes in PAGE-ICE

Assuming the SSP2-4.5 scenario, the mean value of the $SCCO_2$ in 2020 (expressed in $2015 USD throughout) from the previous version of the model, PAGE09, is $158 (figure 2). We note this is greater than the $SCCO_2$ mean value of $106 previously reported for PAGE09 (Hope 2013) due to the use of the SSP2-4.5 scenario instead of SRES A1B (22% increase) and the change in monetary units (23% increase from inflation). We break down the remaining changes from PAGE09 to PAGE-ICE into a series of key steps (figure 2). (a) Updating the CO_2 model, climate sensitivity, and other climate parameters to conform to IPCC AR5, increases the mean $SCCO_2$ to $217. (b) Applying a fat-tailed (Gamma) distribution to sea-level rise increases mean $SCCO_2$ to $228. (c) The permafrost feedback, represented in PAGE-ICE through both CO_2 and CH_4 cycles, increases it to $244. (d) Modeling non-linear transitions in the sea ice and land snow albedo feedback slightly reduces the $SCCO_2$ to $239. (e) We reduce the size, threshold, and lag of discontinuity impacts, since Arctic feedbacks and catastrophic sea level rise are now explicitly modeled, reducing the mean $SCCO_2$ slightly to $213. (f) PAGE-ICE has a longer simulation period (until 2300), which further increases the mean $SCCO_2$ to $239. (g) The baseline income levels, used for calibrating vulnerability, are updated to those observed in 2015, increasing mean $SCCO_2$ to $245. (h) Adjusting the vulnerability of regions in PAGE-ICE to market and non-market damages to be common and equal to the vulnerability of the European Union region increases the mean $SCCO_2$ to $281. Finally, (i) by changing damages to empirical estimates (Burke *et al* 2015) imposed as non-persistent changes to GDP, the final mean $SCCO_2$ for PAGE-ICE is calculated as $307 per tonne.

The uncertainty range is considerable, with an interquartile range of $147–$349, and a 5%–95% range of $82–$831, based on 50 000 Monte Carlo simulations. Nevertheless, for the SSP2-4.5 scenario a clear increase in the $SCCO_2$ is shown, with PAGE-ICE having a mean $SCCO_2$ that is double the value for PAGE09. Strikingly, this increase can be attributed almost entirely to increased social costs in the Global South. The mean $SCCO_2$ attributed to the Global North sees no notable change, mainly due to the regional empirical damage estimates in PAGE-ICE, which allows for benefits of global warming in cooler regions and comes with higher damages in warmer regions compared to the temperature damage function in PAGE09.

3.2. Persistence of economic damages

Based on panel regression analysis using historical temperature and GDP data (Burke *et al* 2015), we estimate that on average 50.1% (34.5%–69.0%, interquartile range) of GDP damages persist as impacts on growth (appendix B.3). Introducing this empirically derived level of damage persistence affects both the size of global GDP and its regional distribution by vast amounts, dominating the effect of any other modeling choice. This impact is a result of deteriorating growth trajectories, particularly in Africa, South Asia, and Latin America. In contrast, cooler regions such as Eastern Europe and Northern Asia ('Russia+') and the European Union (EU)

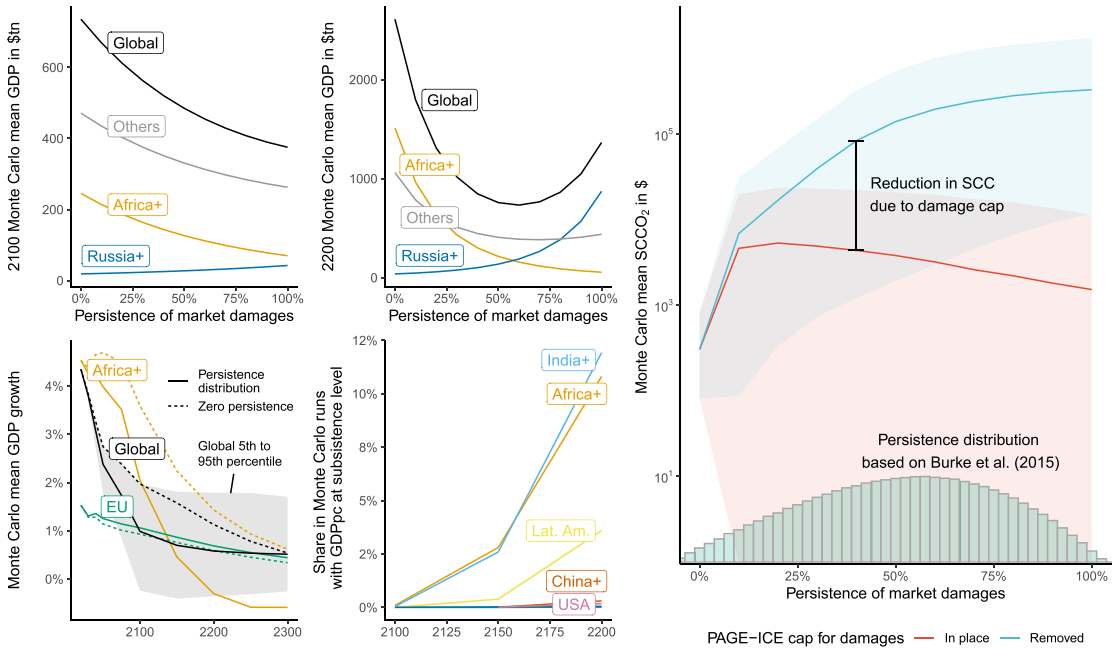

Figure 3. The results of incorporating growth effects into PAGE-ICE, calculated for SSP2-RCP4.5. (a), (b) Mean gross domestic product (GDP) in 2100 and 2200 of the world (black line) and selected regions (colored lines) across fixed values of damage persistence (0%–100%). (c) Mean GDP growth rates of the world (black line) and selected regions (colored lines) for zero persistence and our empirical persistence distribution derived from Burke *et al* (2015) (see appendix B). The grey area indicates the global 5th–95th percentile. (d) Share of Monte Carlo simulations for which a given region reaches the lower bound for GDP per capita during 2100–2200 for our empirical persistence distribution. The subsistence level is derived from the World Bank's international poverty line (see appendix B). Regions that are not displayed (EU, Russia+, and Other OECD) do not reach the subsistence level in any Monte Carlo simulation during this period. (e) $SCCO_2$ of an incremental CO_2 pulse in 2020 across fixed values of damage persistence (0%–100%), with PAGE-ICE's cap for total climate change damages in place or removed (red or blue line, respectively). The shaded areas indicate the 5th–95th $SCCO_2$ percentile. The green bars illustrate our empirical persistence distribution, with frequencies rescaled for illustrative purposes.

experience additional growth. Through the growth rate feedback, these GDP impacts accumulate over time and thus the introduction of damage persistence leads to a considerable redistribution of income to the detriment of poorer regions, an effect which is exacerbated over time. To identify the implications of different levels of persistence on GDP outcomes, we present results both for various fixed degrees of persistence from 0% to 100% (figures 3(a) and (b)) and for our empirically derived persistence distribution (figures 3(c) and (d)).

For this persistence distribution, mean global GDP in 2100 is 30% lower than the SSP2-4.5 growth path without persistence[10]. By 2200, the mean growth loss due to the persistence of climate impacts under SSP2-4.5 exceeds the GDP growth rate in the whole Global South, causing economic contraction. However, the share of runs of negative growth on a global scale as early as 2100 exceeds 8%. By 2200, the 'India+', 'Africa+' and 'Latin America' regions reach income levels associated with extreme poverty in 12%, 11% and 4% of Monte Carlo simulations, respectively. In contrast, mean economic output in the 'Russia+' region is 52% higher with the possibility of Russia+ dominating the global economy near the end of the model horizon for high persistence levels.

If a mere 10% of economic damages were to persist via reduced growth, we find a fifteenfold increase in the mean $SCCO_2$ (figure 3(e)). For higher levels of persistence, however, model estimates of the $SCCO_2$ are found to decrease. This effect is caused by the total climate damages in PAGE being capped to the exogenous statistical value of society ($\$6.13 \times 10^{16}$ following Yumashev *et al* 2019). For high levels of damage persistence, the projected damages go beyond this predefined limit of the model, such that an additional tonne of CO_2 leads to no increase in overall damages and the $SCCO_2$ becomes zero, while the effects of climate change are actually catastrophic in these runs (Weitzman 2014).

Although this is the case in more than half of the Monte Carlo simulations under our empirical persistence distribution, we still estimate a mean $SCCO_2$ of [Line:91 Col:11763372 which exceeds the estimate without damage persistence by an order of magnitude. Performing a sensitivity analysis shows that this estimate is highly sensitive to equity weighting parameters and also varies across methodologies to

[10] Note that for Monte Carlo means of absolute GDP, we omit one outlier run with a persistence draw of −6406%, for which temperature increases push most regions on extremely high growth trajectories, severely distorting the Monte Carlo mean. We only do this for absolute GDP values since trimming this run would have a negligible impact on mean global GDP growth and the $SCCO_2$, reducing the former by 0.003 percentage points or less across years and increasing the latter by $0.07.

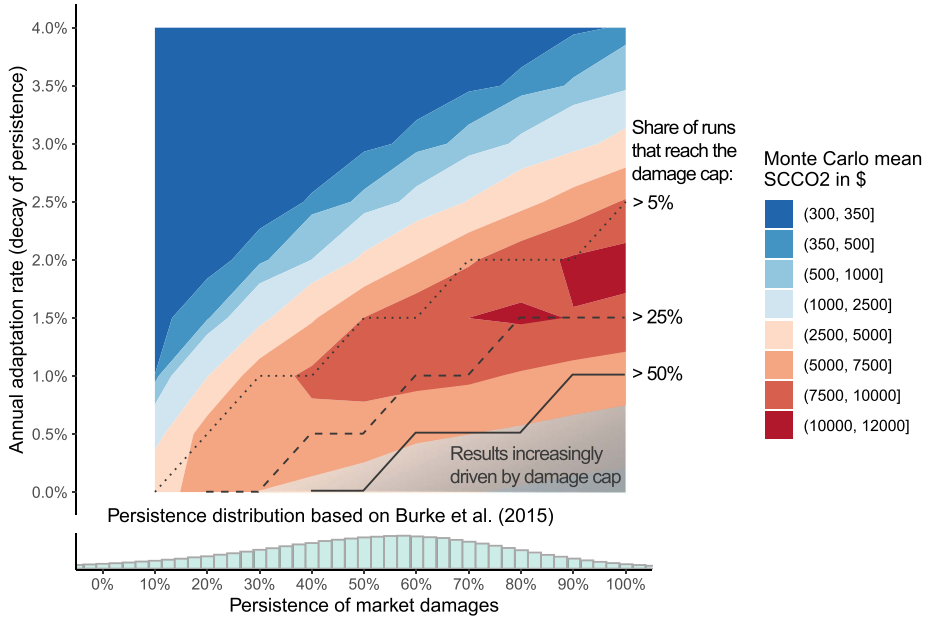

Figure 4. The effect of adaptation reducing the damage persistence over time, calculated for SSP2-RCP4.5. $SCCO_2$ of an incremental CO_2 pulse in 2020 for our empirical persistence distribution, with PAGE-ICE's cap for total climate change damages in place. For all parameter combinations above the dotted, dashed and solid black line, Monte Carlo runs that reach the damage cap and produce $SCCO_2$ estimates of zero account for less than 5%, 25% and 50% of the total 50 000 runs, respectively. Model results are calculated for 10% and 0.5% steps in the persistence and adaptation rate respectively, and then interpolated for plotting purposes. The bottom-right corner is greyed out to highlight that $SCCO_2$ results are primarily driven by the effects of the damage cap.

estimate persistence (appendices B.2 and B.4). The substantial increase in the $SCCO_2$ is primarily driven by the adverse implications for the Global South. Therefore, the resulting $SCCO_2$ is very similar if only lower-income regions are assumed to suffer from persistent economic damages (appendix B.5).

Both current temperature-induced economic damages and the persistence of damages are derived from historical data which do not show an increase in resilience to temperature shocks over time (Burke *et al* 2015, Burke and Emerick 2016). As a result, our approach implicitly assumes that future adaptation will remain at the levels observed hitherto for economic damages. Yet, while there is no clear evidence for adaptation to the market impacts of climate change, it seems unlikely that countries would not invest considerable resources in reducing the lasting effects of temperature increases if actual damages in the (far) future were as big as simulated. Therefore, we further explore the effects of adaptation reducing the damage persistence by a constant annual rate, similar to Moore and Diaz (2015). As figure 4 shows, if current persistence is around 50% (as suggested by the mean of our empirical distribution), then the level of persistence would need to decrease by more than 2% per year via adaptation efforts to reduce the model's $SCCO_2$ to below $2500. As discussed above, the combination of high persistence and low to no adaptation leads to a substantial share of the Monte Carlo runs producing $SCCO_2$ estimates of zero, meaning that the methodological decision behind PAGE-ICE's damage cap increasingly dominates the model results in the lower-right corner of figure 4. Yet, even if current persistence is only 20% and decreases by an annual 0.5%, more than 5% of Monte Carlo reach PAGE-ICE's damage cap and the $SCCO_2$ exceeds $5000. For our empirical persistence distribution, we find that a reduction by at minimum 3% per year would be needed to see a $SCCO_2$ of less than $600 (appendix B.6). In other words, this would require lowering the persistence of temperature-related economic impacts by half within less than 25 years.

3.3. Annual temperature variability

We first implement stochastic annual regional temperatures to the base PAGE-ICE model, and then extend this to the version with persistent climate damages. Variability produces small changes in the means and medians of $SCCO_2$ distributions for all RCP-SSP scenario combinations (figures 5 and 6), with a mean increase of $21 (6.5%) for SSP2-4.5. Accounting for temperature anomalies in model runs leads to a widening of realized temperature ranges, leading to more extreme annual temperatures occurring more frequently, both in the near term and in the long run (figures 5(a) and (b)). This captures better the combination of model uncertainty and internal variability of the climate system for annual global mean temperatures. These wider ranges result in higher mean damages from the non-linear market and non-market damage functions and a greater likelihood of discontinuity damages.

Adding variability also widens the $SCCO_2$ uncertainty ranges. Most of the additional spread of the

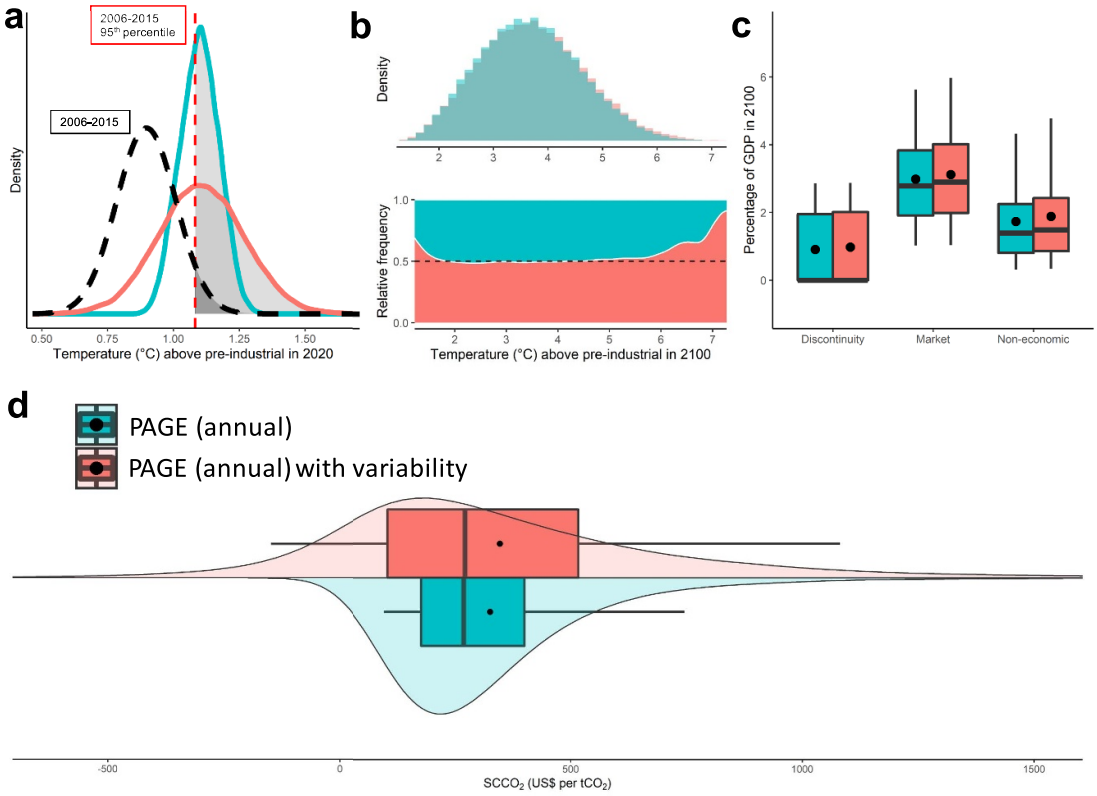

Figure 5. The effects of interannual temperature variability on climate damages for the SSP2-4.5 scenario, assuming no persistence of damages. (a) The modeled temperature distribution in PAGE with (red) and without (blue) variability effects, compared to a density kernel estimate based on historical, linearly detrended global annual mean temperatures for 2006–2015 (dashed, black). Draws with temperatures higher than the 95th historical percentile (dashed, red) are shaded. (b) A histogram of the realized temperature above pre-industrial for the model year 2100, and a relative frequency plot showing the number of PAGE model runs with variability that reach a certain temperature in 2100, divided by the sum of model runs for both model versions that reach that temperature. (c) The effect of variability on projected current damages in 2100 expressed as a percentage of GDP in that year, separately for the three damage modules affected by temperature anomalies. (d) $SCCO_2$ distributions with and without interannual temperature variability. Boxplot error bars indicate the 5th–95th quantile of the distributions, whereas the lines in the box indicate the 25th, median, and 75th quantiles. Means of distributions are shown by a point inside the boxplot.

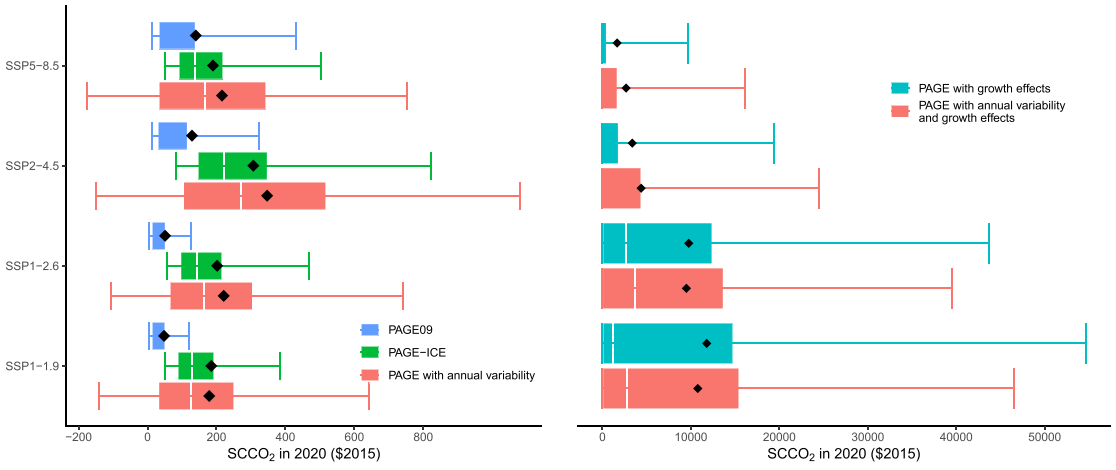

Figure 6. Boxplots of $SCCO_2$ values based on 50 000 Monte Carlo runs of five PAGE model configurations using selected climate and socioeconomic scenario combinations. $SCCO_2$ results for (a) PAGE09, PAGE-ICE, and PAGE with interannual temperature variability, and for (b) PAGE-ICE with growth effects, and PAGE with both growth effects and interannual variability. The whiskers of the boxplots show the 5th and 95th percentile, while the box indicates the interquartile range. Medians are indicated by a white bar, while mean values are indicated by a black diamond. Results reported here are based on data within the 99 percentile range from the 0.5th to the 99.5th percentile. For all SCC values, see appendix table A4.

$SCCO_2$ distributions is explained by the interaction of temperature variability with the convex empirical temperature-damage function used for market damages. The introduction of this symmetric temperature variation widens tails at both ends of the $SCCO_2$ distributions, with the possibility of $SCCO_2$ values

being negative due to regionally beneficial temperature draws in the short term. Introducing the temperature anomalies to an annual version of PAGE with constant damage persistence does not result in an increase in the mean $SCCO_2$ because of the damage cap.

3.4. Alternative climate and socioeconomic scenarios

For the SSP1-1.9 scenario, all model specifications without growth effects produce lower values of the mean $SCCO_2$ compared to SSP1-2.6 and SSP2-4.5. This scenario features the same socioeconomic projections as SSP1-2.6, but with stronger emissions abatement. PAGE with annual variability shows most clearly how more stringent climate mitigation leads to reduced tail risks. For all scenarios, except SSP1-1.9, including the possibility of warm and cold years and periods disproportionately pushes the 75th percentile further from the median than it affects the 25th percentile, while the 5th and 95th percentile are affected more symmetrically. Thus, the consideration of temperature variability increases extremes on both ends, as well as correcting the most likely values upward (figure 6).

For all the PAGE-ICE-based model specifications, we find higher mean values for SSP2-4.5 than for SSP5-8.5. While the projected climate forcing and subsequent impacts are higher for the RCP8.5 scenario, SSP5 projects higher GDP projections than SSP2, leading to a stronger discounting of future damages, producing lower $SCCO_2$ values in PAGE-ICE. Moreover, because radiative forcing is logarithmic in concentration (Shine *et al* 1990), marginal impacts are reduced for higher emission trajectories. For SSP1-2.6, climate change-induced damages are much lower compared to SSP2-4.5, leading to significantly lower $SCCO_2$ values if no damage persistence is considered. The $SCCO_2$ values for model versions with growth effects for different scenarios are driven by model runs reaching the damage cap, explaining the lower values for pathways with higher emissions when damages are likely to be higher.

4. Discussion and conclusions

Our results show that determining the level of persistence of economic damages is one of the most important factors in calculating the $SCCO_2$, and our empirical estimate illustrates the urgency of increasing adaptive capacity, while suggesting that the mean estimate for the $SCCO_2$ may have been strongly underestimated. It further indicates that considering annual temperature anomalies leads to large increases in uncertainty about the risks of climate change. Differences between PAGE09 and PAGE-ICE show that the previous $SCCO_2$ results have also decidedly underestimated damages in the Global South.

The implemented climate feedbacks and annual mean temperature variability do not have large effects on the mean $SCCO_2$. The inclusion of permafrost thawing and surface albedo feedbacks is shown to lead to a relatively small increase in the $SCCO_2$ for SSP2-4.5, with modest distributional effects. Consideration of temperature anomalies shows that internal variability in the climate system can lead to increases in $SCCO_2$ estimates, and is key to understanding uncertainties in the climate-economy system, stressing the need for a better representation of variability and extremes in CB-IAMs.

Including an empirical estimate of damage persistence demonstrates that even minor departures from the assumption that climate shocks do not affect GDP growth have major economic implications and eclipse most other modeling decisions. It suggests the need for a strong increase in adaptation to persistent damages if the long-term social cost of emissions is to be limited. Our findings corroborate that economic uncertainty is larger than climate science uncertainty in climate-economy system analysis (Van Vuuren *et al* 2020), and provide a strong argument that the assumption of zero persistence in CB-IAMs should be subject to increased scrutiny in order to avoid considerable bias in $SCCO_2$ estimates. A better understanding of the persistence of damages and potential adaptation mechanisms is key for deriving more accurate $SCCO_2$ estimates, and the issue of damage persistence should receive similar attention as other key $SCCO_2$ determinants, like the discount rate or climate sensitivity.

Due to data limitations, this study used a global model of damage persistence with no regional disaggregation. Therefore, its main results do not see heterogeneous responses to warming, which risks the omission of potentially substantial inequalities caused by the altered long-run growth pathways. Further research and process-based modeling assessments are required to quantify climate-driven growth effects along sectoral, spatial and temporal dimensions. Given that our results are mainly driven by persistence effects on warmer regions with lower income levels, future research should in particular focus on advancing the understanding of growth effects in the Global South and on tackling them.

Data availability statement

The data that support the findings of this study are openly available at the following URL: https://zenodo.org/record/3907851. DOI: 10.5281/zenodo.3907851.

Code and data availability

Model code and documentation is available from the GitHub repository, https://github.com/openmodels/MimiPAGE2020.jl, DOI: https://zenodo.org/record/5081138#.YRTfXa9Khyw.

Acknowledgments

Supported by the H2020-MSCA-RISE project GEMCLIME-2020 GA No. 681228. This work has been supported by the Natural Environment Research Council under Grant Agreement NE/S007415/1. J S K acknowledges support from stichting dr Hendrik Muller's Vaderlandsch Fonds and Meindert Douma Leen. The views expressed in this paper do not necessarily reflect the views of NERA Economic Consulting.

Author contributions

J S K, J R, C M B conceived and implemented annual temperature variability in PAGE, P W, J R, J S K implemented growth effects and analyzed the respective results, J R, C H, D Y analyzed the differences between PAGE09 and PAGE-ICE. J S K, J R, P W wrote the manuscript and performed the model experiments. All authors reviewed the manuscript.

Conflict of interest

P W advised companies in the energy sector whose net income would be affected if new findings on the $SCCO_2$ were to translate into policies aiming for higher carbon prices. The remaining authors declare no competing interests.

Appendix A. Model choices, model information, summary statistics, and sensitivities in calculating the $SCCO_2$ for PAGE

A.1. Model regions

A.2. CO_2 pulse size to calculate the $SCCO_2$

To estimate the marginal damage of an additional tonne of CO_2, PAGE is run twice, with one run based on the exogenous emission scenario and the second run adding a CO_2 pulse in the first model time step in 2020, which ranges from mid-2017 to 2025. This requires a decision regarding the time and the size of the said pulse. While a pulse of merely one tonne of CO_2 captures a truly marginal effect, larger pulse sizes are typically used (Otto *et al* 2013, Rose *et al* 2017). The results displayed in figure A2 show that the $SCCO_2$ is more stable for pulses that are not truly marginal. While small pulses are too variable and sensitive for the specific model and pulse size setting, larger pulse sizes do not accurately capture marginal damages and could see unexpected slight increases in the $SCCO_2$ as seen for PAGE-ICE around 100 Gt. This increase, which is still well within the confidence interval, might be attributed to the triggering of a discontinuity effect. To strike a balance, all our $SCCO_2$ estimates are based on an annual pulse size of 10 Gt of CO_2 in model year 2020, totalling a 75 Gt CO_2 pulse over the period modeled.

A.3. Sensitivity analysis of the $SCCO_2$

A.4. Extending the SSP timeseries

To estimate population and income levels past 2100, we fit a model to the available SSP data and extrapolate it. Both population and income use the same model, defined in terms of growth rates. The model postulates that the changes in growth rates are explained by a rate of convergence and a rate of decay.

The model is as follows:

$$\begin{aligned}\text{Growth}_{i,t} = (1-\beta-\delta)\text{Growth}_{i,t-1} \\ + \delta\text{MeanGrowth}_{t-1}\end{aligned}$$

where i indexes the region, t indexes years, and $\text{MeanGrowth}_{t-1} = \sum_i \frac{\text{Population}_{i,0}}{\sum_i \text{Population}_{i,0}}\text{Growth}_{i,t-1}$. Above, δ is the rate of convergence, and β is the decay rate.

As SSP data are not available for every year, fitting the exact expression above requires a model with dynamics. We use a two-step approach, fitting the model using Stan, a computational Bayes system. The first step uses the available data directly, fitting the following

$$\begin{aligned}\text{Growth}_{i,s} \sim \mathcal{N}(\text{Growth}_{i,s-1}(1-\Delta t(\beta+\delta)) \\ + \text{MeanGrowth}_{s-1}\Delta t\delta, \sigma_i)\end{aligned}$$

where s indexes time-steps, Δt is the number of years between time-steps, and country i has uncertainty σ_i. We apply a prior that both β and δ are between 0 and 0.5.

Next, we fit the full model, using the results of the simplified model to improve the Bayesian model convergence. In this case, for a given MCMC draw of β and δ, we calculate the entire time series:

$$\begin{aligned}\widehat{\text{Growth}}_{i,t} \sim \mathcal{N}\left(\widehat{\text{Growth}}_{i,t-1}(1-\beta-\delta)\right. \\ \left.+(\widehat{\text{Growth}}_{i,t-1}\cdot w_i)\delta, \sigma_i\right)\end{aligned}$$

starting with $\widehat{\text{Growth}}_{i,0}$ as known from the SSP dataset.

The probability evaluation is over both the performance of the fit and the priors:

$$\begin{aligned}\text{Growth}_{is} \sim \mathcal{N}\left(\widehat{\text{Growth}}_{i,t(s)}, \sigma_i\right) \\ \beta \sim \mathcal{N}(\mu_\beta, \sigma_\beta) \\ \delta \sim \mathcal{N}(\mu_\delta, \sigma_\delta) \\ \log\sigma_i \sim \mathcal{N}(\mu_{\sigma,i}, \sigma_{\sigma,i})\end{aligned}$$

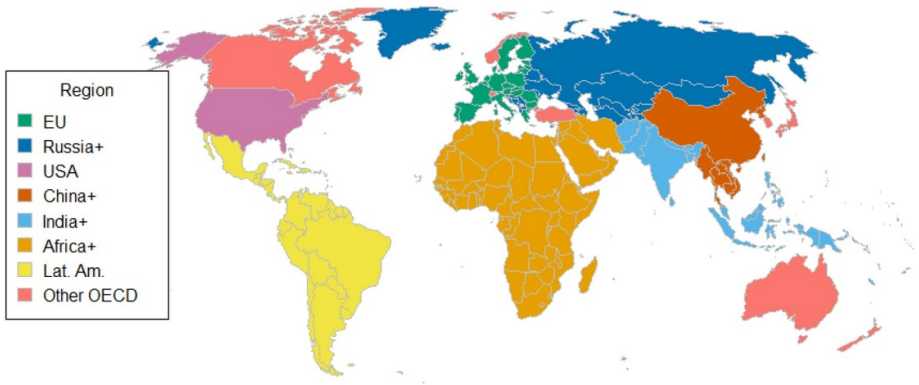

Figure A1. Regions as modelled in PAGE-ICE, based on information from Yumashev *et al* (2019).

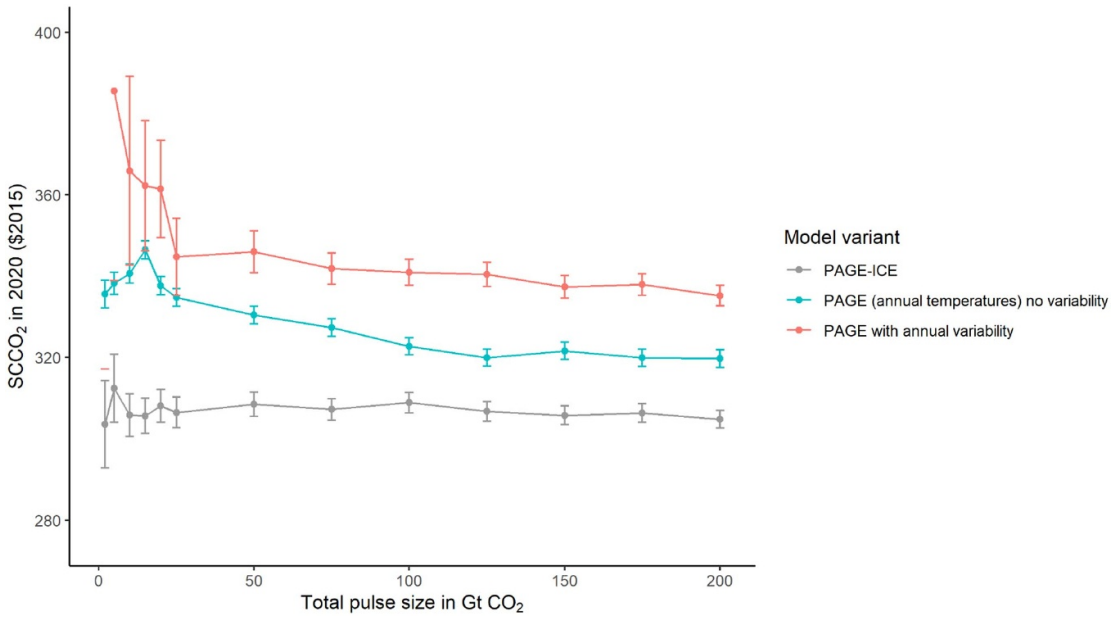

Figure A2. The mean with confidence intervals for the $SCCO_2$ based on 50 000 Monte Carlo runs for selected model variants PAGE-ICE, PAGE with only annual temperatures but no variability, and PAGE with annual temperatures and annual variability, for varying pulse sizes (total shock in Gt) for SSP2-4.5.

where $\mu_.$ is the mean estimate for the corresponding parameter, and $\sigma_.$ is the standard deviation across its uncertainty. The prior for σ_i is defined as a log-normal, centered on the mean of the estimates of log σ_i.

The estimates for each SSP are shown below (table A3), with visualizations of time series data for SSP2 and SSP5 in figure A5.

A.5. Additional $SCCO_2$ results

In addition to the results presented in the main text, we have run all different model versions for four separate scenarios (table A4).

A.6. Annualization of a modular framework

The PAGE model is composed of several modules for increased functionality and increased flexibility for future development and specific applications, and is based on Mimi-PAGE (Moore *et al* 2018) and PAGE-ICE (Yumashev *et al* 2019). To introduce annual temperature variability, an annual temperature model is required, and hence all downstream and related upstream modules involved in the climate-economy feedback were annualized. This was done by exponentially interpolating between PAGE-ICE time steps for population, sea level, and abatement costs, and linearly interpolating GDP and emissions growth rates. These choices are made to stay as close to the original design as possible. An annual model comes with reduced modeling artefacts that plague models with multi-year time steps. In non-annual models, rather than having smooth damage distributions, one finds multimodal damage distributions for binary damage elements, for instance in discontinuity damages modules where damages can only be triggered in the chosen model years, rather than

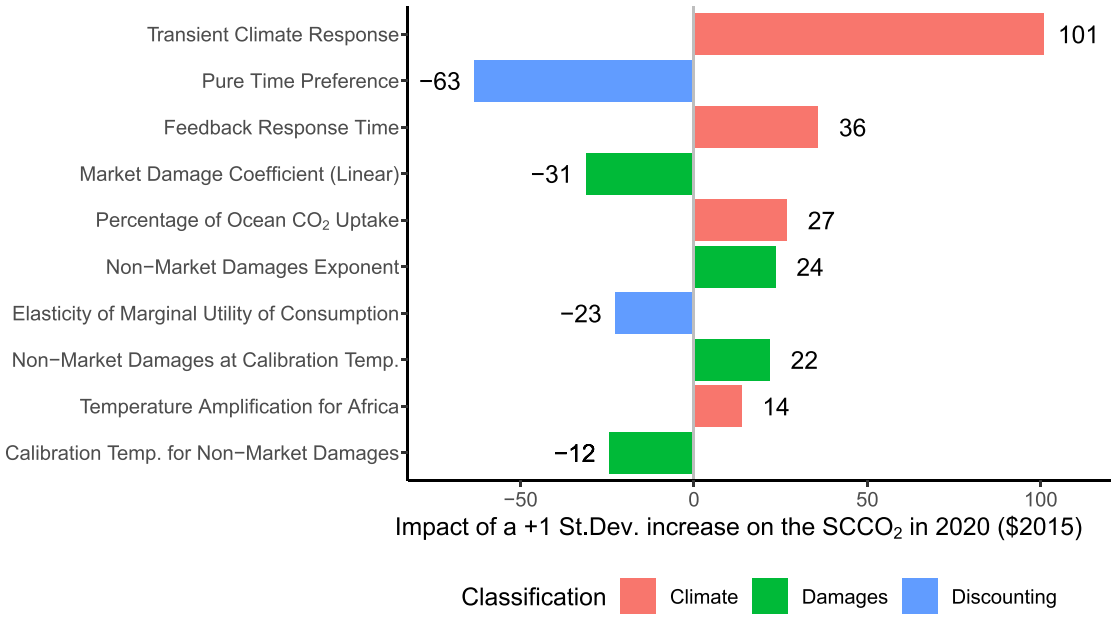

Figure A3. Impact of a parameter *increase* by one standard deviation on the 2020 $SCCO_2$ based on the default PAGE-ICE model for SSP2-4.5 (deterministic run). The $SCCO_2$ impact is calculated as the difference between the $SCCO_2$ for the mean of the respective parameter's Monte Carlo distribution, and the $SCCO_2$ for a parameter value equal to the mean value increased by one standard deviation, while all other parameters remain at their default value. Only parameters with an absolute $SCCO_2$ impact of at least $10 are displayed here.

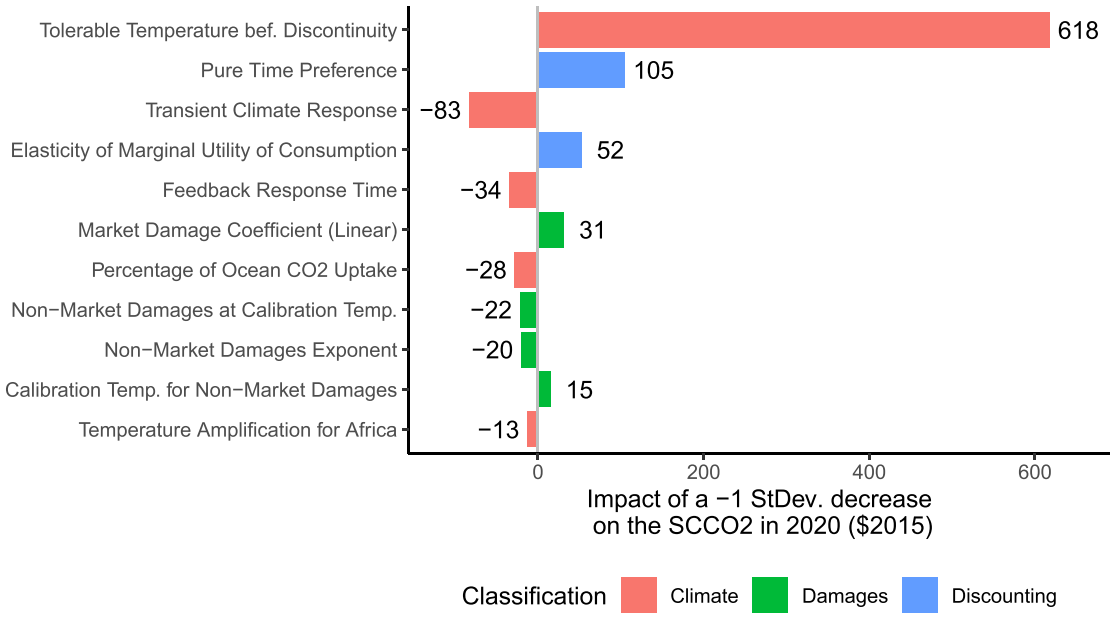

Figure A4. Impact of a parameter *decrease* by one standard deviation on the 2020 $SCCO_2$ based on the default PAGE-ICE model for SSP2-4.5 (deterministic run). The $SCCO_2$ impact is calculated as the difference between the $SCCO_2$ for the mean of the respective parameter's Monte Carlo distribution, and the $SCCO_2$ for a parameter value equal to the mean value increased by one standard deviation, while all other parameters remain at their default value. Only parameters with an absolute $SCCO_2$ impact of at least $10 are displayed here. Note that a one standard deviation decrease in the tolerable temperature before a discontinuity occurs triggers the discontinuity in this particular case, thus leading to a substantial increase in the $SCCO_2$.

any year modeled. Our annual model reports $SCCO_2$ distributions that differ from the original model. This is due to changes in the discontinuity sector and the model design of PAGE09 where each time step year covers half of the time to the next analysis year.

Table A1. Impact of a parameter *increase* by one standard deviation on the 2020 $SCCO_2$ based on the default PAGE-ICE model for SSP2-4.5 (deterministic run). The $SCCO_2$ impact is calculated as the difference between the $SCCO_2$ for the mean of the respective parameter's Monte Carlo distribution and the $SCCO_2$ for a parameter value equal to the mean value decreased by one standard deviation, while all other parameters remain at their default value. Only parameters with an absolute $SCCO_2$ impact of at least $2 are displayed here.

	Model parameter	Impact on the $SCCO_2$ in 2020 ($2015)
1	tcr_transientresponse	100.88
2	ptp_timepreference	−63.29
3	frt_warminghalflife	35.77
4	impf_coeff_lin	−31.06
5	a1_percentco2oceanlong	26.78
6	pow_NonMarketExponent	23.51
7	emuc_utilityconvexity	−22.63
8	w_NonImpactsatCalibrationTemp	21.84
9	ampf_amplification_Africa	13.68
10	tcal_CalibrationTemp	−12.15
11	iben_NonMarketInitialBenefit	9.21
12	stay_fractionCO2emissionsinatm	8.84
13	ampf_amplification_SEAsia	6.61
14	ipow_NonMarketIncomeFxnExponent	5.91
15	sltau_SLresponsetime	−4.32
16	W_SatCalibrationSLR	4.16
17	pow_SLRImpactFxnExponent	4.12
18	sltemp_SLtemprise	4.05
19	rtl_abs_0_realizedabstemperature_Africa	3.73
20	ind_slopeSEforcing_indirect	2.77
21	ipow_MarketIncomeFxnExponent	2.71
22	t2_timeco2oceanshort	2.67
23	rtl_abs_0_realizedabstemperature_SEAsia	2.16

Table A2. Impact of a parameter *decrease* by one standard deviation on the 2020 $SCCO_2$ based on the default PAGE-ICE model for SSP2-4.5 (deterministic run). The $SCCO_2$ impact is calculated as the difference between the $SCCO_2$ for the mean of the respective parameter's Monte Carlo distribution and the $SCCO_2$ for a parameter value equal to the mean value decreased by one standard deviation, while all other parameters remain at their default value. Only parameters with an absolute $SCCO_2$ impact of at least $2 are displayed here. Note that a one standard deviation decrease in the tolerable temperature before a discontinuity occurs triggers the discontinuity in this particular case, thus leading to a substantial increase in the $SCCO_2$.

	Model parameter	Impact on the $SCCO_2$ in 2020 ($2015)
1	tdis_tolerabilitydisc	617.53
2	ptp_timepreference	104.61
3	tcr_transientresponse	−82.96
4	emuc_utilityconvexity	52.43
5	frt_warminghalflife	−34.02
6	impf_coeff_lin	31.19
7	a1_percentco2oceanlong	−27.95
8	w_NonImpactsatCalibrationTemp	−21.64
9	pow_NonMarketExponent	−20.11
10	tcal_CalibrationTemp	14.99
11	ampf_amplification_Africa	−12.77
12	iben_NonMarketInitialBenefit	−9.19
13	stay_fractionCO2emissionsinatm	−9.04
14	ampf_amplification_SEAsia	−6.30
15	sltemp_SLtemprise	−5.88
16	ipow_NonMarketIncomeFxnExponent	−5.01
17	W_SatCalibrationSLR	−4.14
18	sltau_SLresponsetime	3.93
19	rtl_abs_0_realizedabstemperature_Africa	−3.73
20	pow_SLRImpactFxnExponent	−3.58
21	ind_slopeSEforcing_indirect	−3.13
22	t2_timeco2oceanshort	−2.81
23	rtl_abs_0_realizedabstemperature_SEAsia	−2.15
24	ipow_MarketIncomeFxnExponent	−2.07

Table A3. Population and income extension model parameters.

SSP	Variable	δ	β
1	GDP per capita	0.006205028	0.005930520
1	Population	0.008967453	0.005215835
2	GDP per capita	0.004190444	0.007228942
2	Population	0.001276993	0.011064426
3	GDP per capita	0.006273030	0.009597363
3	Population	0.001064697	0.007688331
4	GDP per capita	0.006895296	0.009651277
4	Population	0.001867587	0.003461600
5	GDP per capita	0.007766807	0.003843256
5	Population	0.003470952	0.004305310

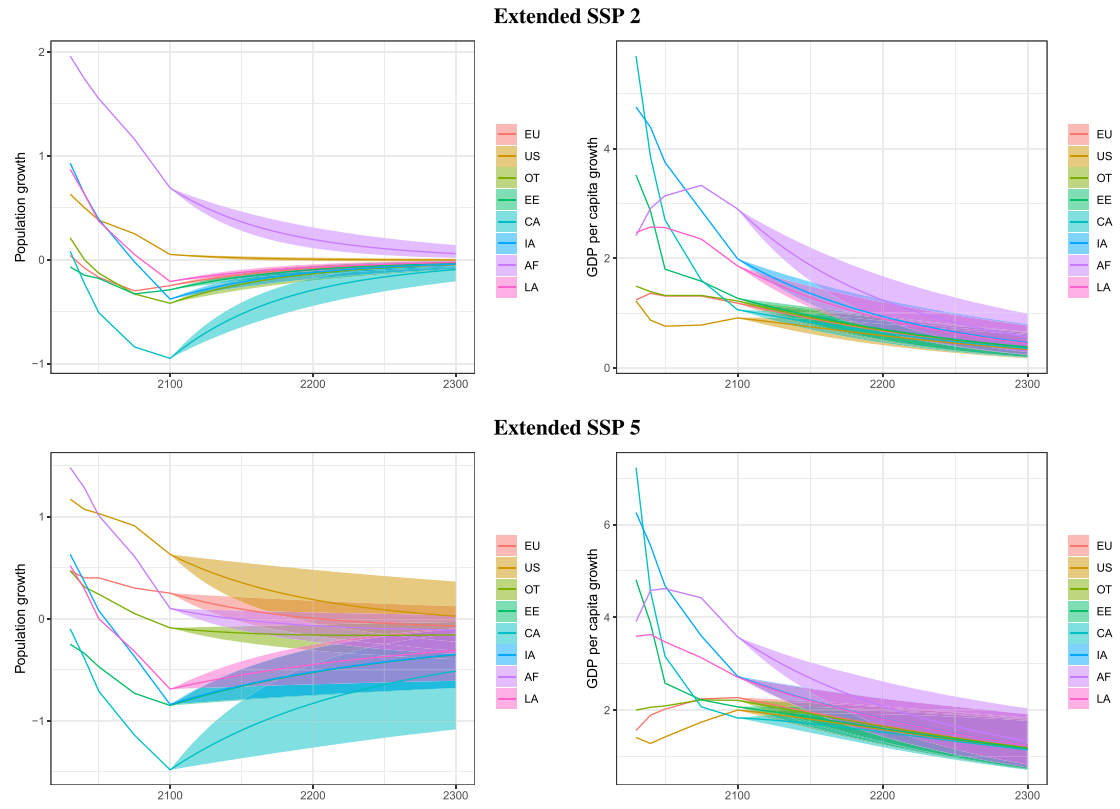

Figure A5. Extended SSP population and per capita GDP for SSP 2 and SSP 5. Shaded areas show 95% credible intervals.

Table A4. Mean (25th–75th [5th–95th] percentile) $SCCO_2$ values based on 50000 Monte Carlo runs. The alternative variability model features regional temperatures that vary independently (no autoregression) and includes observational uncertainties on the standard deviations in the Monte Carlo simulations, as described in appendix section C3. Marked (*) values represent statistical values of distributions that include $SCCO_2$ values of zero caused by damages being outside of the predefined scope of the model. Note that for some of the (*) values, extreme Monte Carlo draws for persistence also cause numerical issues in a handful of model runs, which reduces the effective underlying Monte Carlo sample size by less than 0.1%. However, this does not affect our main results for SSP2-4.5. Double marked (**) indicates that in PAGE09 we ran an alternative emissions pathway aligned with staying below 1.5°C rather than using RCP1.9, meaning a slightly higher $SCCO_2$ estimates.

	SSP1-1.9	SSP1-2.6	SSP2-4.5	SSP5-8.5
PAGE09	48 (14–50 [5–121])**	51 (14–51 [5–126])	129 (31–115 [13–323])	140 (35–138 [14–430])
PAGE-ICE	185 (89–192 [51–383])	202 (97–215 [56–469])	306 (148–347 [83–823])	190 (92–217 [51–503])
PAGE with growth effects	11787 (76–14675 [0–54689])*	9760 (66–12373 [0–43722])*	3372 (0–1781 [0–19370])*	1662 (0–426 [0–9704])*
PAGE (annual temperatures) no variability	178 (80–189 [45–382])	214 (107–245 [63–482])	326 (177–400 [97–748])	202 (104–247 [55–488])
PAGE with annual variability	179 (33–250 [−142–643])	221 (67–304 [−105–742])	347 (105–517 [−149–1082])	216 (34–342 [−175–754])
PAGE with alternative annual variability model	176 (61–207 [−22–519])	216 (89–259 [−2–619])	328 (137–449 [−10–902])	202 (72–285 [−40–582])
PAGE (annual) with growth effects	10849 (85–15909 [0–39242])*	9487 (95–14103 [0–31807])*	4439 (0–6871 [0–21093])*	2754 (0–2956 [0–14081])*
PAGE with annual variability and growth effects	10780 (62–15414 [−33–46514])*	9491 (41–13641 [−102–39545])*	4377 (0–4336 [0–24481])*	2675 (0–1647 [0–16109])*

Appendix B. Persistence of damages

As the exact distribution of persistence is unknown, it has been specified in various ways. Dietz and Stern (2015) set it to 0.05 to allow for minimal growth effects only whereas Moore and Diaz (2015) parametrize it based on the relative magnitude between the immediate marginal impact of temperature on GDP growth to the cumulative effect over time, defined as the sum over all lag coefficients. While their estimate relies on Dell *et al* (2012), we apply this methodology to the data by Burke *et al* (2015) but limit ourselves to one lag as introducing further temperature lags primarily adds noise (see appendix B.3).

Since high persistence of damages might cause economic collapse of some regions, equity-weighted damages in utility terms approach infinity if consumption goes to zero. Therefore, we introduce a subsistence bound at a per capita consumption level which equals the current World Bank threshold for extreme poverty (converted to 2015 dollars). As GDP losses compared to a baseline scenario without climate change might still exceed the consumption level actually realized, we further limit equity-weighting to damages less or equal to 99% of consumption. Damages exceeding this threshold are still taken into account but are not subject to equity weights. To avoid the two aforementioned boundaries causing discontinuities in the SCC results, we use a convergence system in the proximity of the thresholds.

B.1. Incorporating growth effects

In PAGE-ICE, economic growth is exogenously specified by:

$$\mathrm{GDP}_{r,t} = \mathrm{GDP}_{r,t-1} \cdot (1 + g_{r,t}) \tag{B1}$$

where $g_{r,t}$ is the SSP-specific growth rate for region r at time step t. Previous work has introduced growth effects as a share of damages affecting capital stocks or total factor productivity, but as such factors are not explicitly modeled in PAGE, we implement a persistence parameter (Estrada *et al* 2015) into the parameterized growth system (Burke *et al* 2015) such that:

$$\mathrm{GDP}_{r,t} = \mathrm{GDP}_{r,t-1} \cdot (1 + g_{r,t} - \rho \cdot \gamma_{r,t-1}) \tag{B2}$$

where ρ specifies the share of economic damages γ that affect the growth rate. If, for instance, market damages equal 2% of GDP, then for $\rho = 0.5$, economic growth decreases by one percentage point. This approach has three advantages. Firstly, it introduces only one additional parameter thus facilitating the specification of its Monte Carlo distribution. Nonetheless, it can easily be adjusted to new research about region-specific vulnerabilities or hypotheses about future developments by differentiating ρ over regions and time. Secondly, it nests both level effects and the growth system by Burke *et al* (2015) for $\rho = 0$ and $\rho = 1$, respectively, and hence covers a range of approaches applied in previous studies. Thirdly, it mirrors the share of damages inflicted upon productivity or capital stocks in

previous papers (Moyer *et al* 2014, Dietz and Stern 2015, Moore and Diaz 2015) which facilitates comparisons. It is important to note, however, that the γ returned by the damage function in Burke *et al* (2015) is expressed in % of GDP per capita, not in % of GDP. By applying γ directly to the GDP growth rate and leaving population exogenous, we assume that the adverse GDP per capita impact of a temperature stems only from a reduced GDP and not from an increase in population, in line with indications that a temperature shock would result in a minor decrease in population (Carleton *et al* 2020).

B.2. Boundaries for economic collapse and equity-weighting

Damage persistence can have catastrophic impacts on the welfare of regions, to the extent that some regions approach zero consumption. Even if this is not the case, counterfactual GDP losses, defined as the difference between counterfactual GDP levels in the absence of climate change and GDP levels actually realized, might still exceed a region's consumption. Both outcomes would lead to infinite equity-weighted damages in utility terms in PAGE. To see this, note that damages are equity-weighted based on a region's consumption level (Anthoff *et al* 2009a) relative to the EU in 2015 such that:

$$\tilde{D}_{r,t} = \frac{C_{\mathrm{EU},2015}^{\eta}}{(1-\eta)} \cdot \left[C_{r,t}^{1-\eta} - (C_{r,t} - D_{r,t})^{1-\eta} \right] \quad \text{(B3)}$$

where $\tilde{D}_{r,t}$ is equity-weighted damages per capita, $C_{r,t}$ and $D_{r,t}$ are unweighted consumption and damages per capita and η is the elasticity of marginal utility of consumption of the underlying iso-elastic welfare function. If $D_{r,t}$ approaches $C_{r,t}$, this expression yields infinitely large values for $\tilde{D}_{r,t}$ and becomes numerically infeasible once $D_{r,t}$ exceeds $C_{r,t}$.

We therefore introduce two boundaries. First, we assume that a region's per capita consumption cannot fall below the World Bank's current threshold for extreme poverty of \$1.90 (2011 PP) per day, converted to \$2015 (PAGE-ICE's monetary unit) using the World Development Indicators' GDP deflator time series. As a result, per capita consumption in the model cannot drop below \$740.65 (per year) which equals about 17% of the 2015 per capita consumption for the poorest region in PAGE-ICE, India+. Furthermore, we assume that only damages which equal up to 99% of a region's per capita consumption are subject to equity-weighting, following Dietz (2011). Damages that exceed this threshold are still taken into consideration but receive no equity weights. Overall damage estimates are highly sensitive to the level of such a threshold (Dietz 2011), a finding corroborated by our sensitivity analysis (see figure B1). In general, total damages increase with increased levels of equity weighting. However, the $SCCO_2$ Monte Carlo mean actually decreases because for higher total damages, more Monte Carlo runs reach PAGE-ICE's upper bound for overall damages and thus produce $SCCO_2$ estimates of zero.

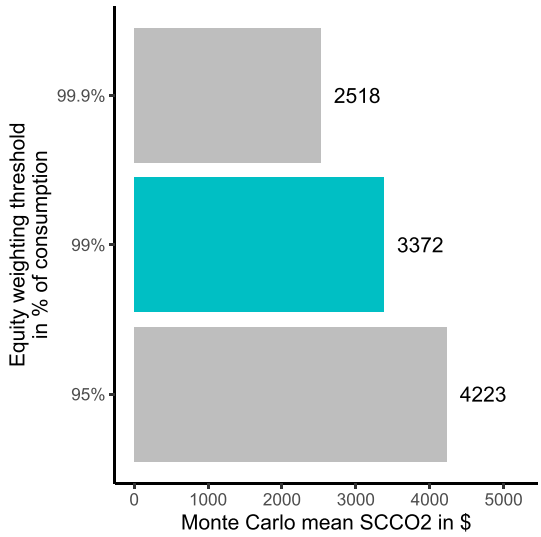

Figure B1. Mean $SCCO_2$ based on 50 000 Monte Carlo under different equity-weighting thresholds for SSP2-4.5. The blue bar marks our default setting.

The two boundaries explained above are likely to cause considerable discontinuities in results. For example, the marginal damages of CO_2 will abruptly decrease once a region reaches the subsistence level of per capita consumption because additional temperature rises cannot depress economic growth further. Similarly, the equity-weighted marginal damages of an additional tonne of CO_2 will be extremely high for a region with damages just below the 99% threshold but will fall abruptly once the threshold is reached. To smooth out these effects, we introduce these boundaries as logistic paths such that the consumption and equity-weighted damages converge against the threshold without fully reaching it. This convergence system is expressed by the following equation:

$$\tilde{y} = \begin{cases} y & \text{if } y \geqslant \epsilon \\ -\theta + \dfrac{2(\theta-\epsilon)\cdot\exp(b(y-\epsilon))}{1+\exp(b(y-\epsilon))} & \text{if } y < \epsilon \end{cases}$$

where y is the original variable subject to threshold θ and $\tilde{y}$ is the adjusted variable converging asymptotically against θ. ϵ is a value close to θ which triggers the converging process, and b is defined as $b = \dfrac{2}{\theta-\epsilon}$.

This system ensures both that $\tilde{y}$ converges against θ as y goes to infinity and that the derivative of $\tilde{y}$ with respect to y equals 1 at $y = \epsilon$, thus avoiding breaks. Figure B2 illustrates the convergence system for the equity-weighting threshold discussed above, which, in our default settings, has an upper bound at $\theta = 0.99$ and convergence starting at a neighborhood value of $\varepsilon = 0.9$. For the per capita consumption threshold, ε equals 1.5 times the subsistence level.

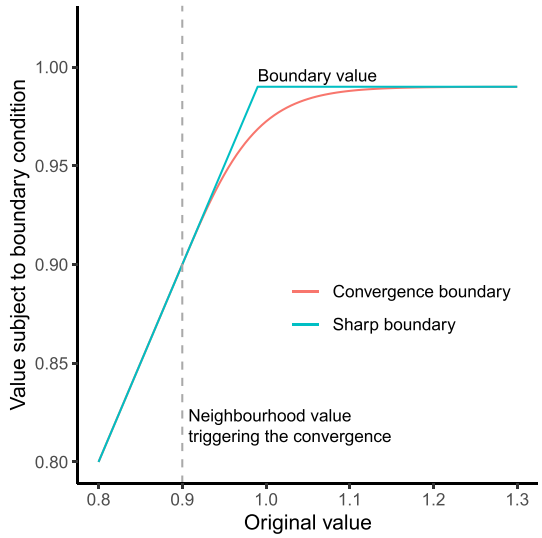

Figure B2. Illustration of the implemented convergence system.

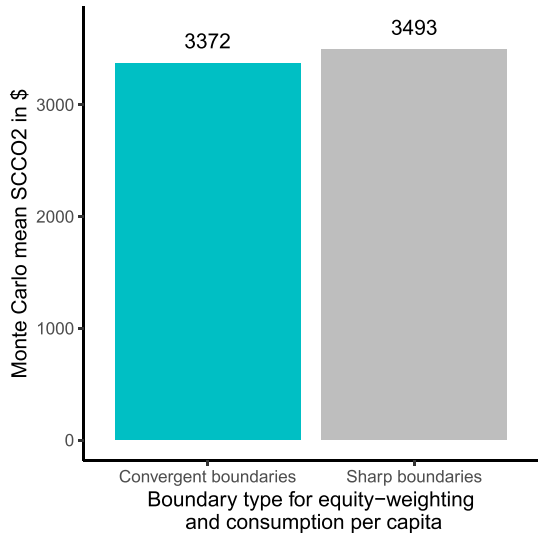

Figure B3. Mean $SCCO_2$ based on 50 000 Monte Carlo under different implementations of the boundary conditions for SSP2-4.5. The blue bar marks our default setting.

Figure B3 shows the impact of the convergence system on the $SCCO_2$ results. In general, the introduction of the convergence system decreases the $SCCO_2$, but the effect is modest compared to other model parameter settings (see for instance figure B1).

B.3. Calibrating the persistence of damages

The previous literature provides two general approaches to determining a point estimate for the persistence of market damages. In some studies, persistence is set to a low, but somewhat arbitrary value to explore growth effects without making strong assumptions regarding the magnitude of persistence (Dietz 2011, Moyer *et al* 2014). The more empirical approach relies on fixed effects regressions of economic growth on various variables, including temperature (Dell *et al* 2012, Burke *et al* 2015). A generic equation for such a model would be

$$g_{i,t} = \beta \text{Temperature}_{i,t} + \gamma \cdot X_{i,t} + \alpha_i + \delta_t + \epsilon_{i,t} \tag{B4}$$

where $g_{i,t}$ denotes the growth rate of country i at time t and $X_{i,t}$ denotes a vector of additional independent variables with the vector of coefficients γ. If not all of the damages indicated by β persist over time and the economy eventually returns to its original growth trajectory, then a negative GDP impact at time t is followed by a compensating impact in the subsequent years. This can be conceptualized by introducing a lag into the model equation:

$$g_{i,t} = \beta_1 \text{Temperature}_{i,t} + \beta_2 \text{Temperature}_{i,t-1} + \gamma \cdot X_{i,t} + \alpha_i + \delta_t + \epsilon_{i,t}. \tag{B5}$$

If damages are not fully persistent over time, then signs of β_2 will be positive. If, on the other hand, damages only reach their full extent over time (e.g. because some damages to infrastructure is exacerbated over time), the sign of β_2 will be negative as well. Of course, there is no imminent reason to assume that the full effects of a temperature shock are realized after only one year. Therefore, researchers typically include further lags into the equation and estimate the long-run marginal impact of temperature on growth (Dell *et al* 2012, Moore and Diaz 2015), which can identify damage persistence ρ based on its ratio to the immediate marginal impact. Note that for a model with k lags, such a ratio is defined as follows:

$$\rho = \frac{\sum_{j=1}^{k} \beta_j}{\beta_1}. \tag{B6}$$

In the case of pure level effects, all immediate impacts of temperature shocks are compensated for over time and the numerator of $\rho = 0$ becomes zero. If, however, after k years, the long-run marginal impact is only half the immediate impact of a temperature shock, we can conclude that only 50% of economic damages persist over time. Yet, unlike the simple model given in equation (B4), the regression model by Burke *et al* (2015) which informs PAGE's market damage function is quadratic in temperature:

$$g_{i,t} = \beta_{1,0} \cdot \text{Temperature}_{i,t} + \beta_{2,0} \cdot \text{Temperature}^2_{i,t} + \gamma \cdot X_{i,t} + \alpha_i + \delta_t + \epsilon_{i,t}. \tag{B7}$$

This means that the marginal impact of temperature depends on the initial temperature. Hence, there is no universal ratio of long-run to immediate impacts

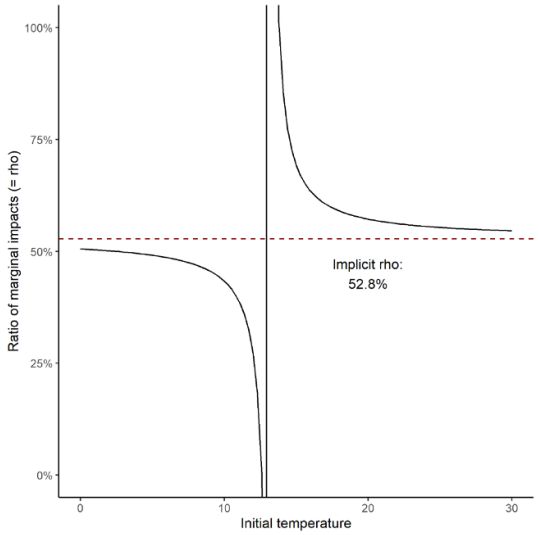

Figure B4. Ratio of long-run to immediate marginal impact using the Burke *et al* (2015) regression with one temperature lag.

for all regions but for a model with k lags, ρ is defined as follows:

$$\rho = \frac{\sum_{j=0}^{k} \beta_{1,j} + 2\beta_{2,j} \cdot \text{Temperature}_{i,t}}{\beta_{1,0} + 2\beta_{2,0} \cdot \text{Temperature}_{i,t}}. \quad \text{(B8)}$$

However, the variation of ρ can be understood as a numerical, rather than theoretical, issue. To see this, note that in the case of a quadratic regression model, both the long-run and the immediate marginal impacts are linear functions of temperature. The immediate marginal impact, which is the denominator of ρ, approaches zero around 13°C for the coefficients from Burke *et al* (2015), leading to a damage persistence of $\pm\infty$ in the proximity of this temperature (see figure B4). Therefore, there is little use in aggregating the ratio of marginal impacts for different temperatures, e.g. by using population weights. Asymptotically, however, the ratio becomes numerically stable, as illustrated by figure B4. For this reason, we estimate the damage persistence as the ratio of long-run to immediate marginal impacts as the temperature goes to (minus) infinity, as indicated by the lagged regression model by Burke *et al* (2015).

The question remains as to how many temperature lags one should include in the regression model. Ideally, we would include as many lags as possible to avoid a bias in our ρ estimate due to omitted future rebounds or, conversely, intensification of damages. In practice, however, every lag added to the model comes with a considerable amount of variance, such that the ρ estimate loses its meaning if too many imprecisely estimated lag coefficients are included. For this reason, we rely on the specification with only one lag, for which the quadratic lag coefficient is significant at the 5%-level, while the linear lag coefficient is not (see table B1). As the signs of the first temperature lag are opposite to the immediate temperature impact, the resulting damage persistence equals only 52.8% of the immediate impact.

The numerator and denominator of ρ are linear combinations of asymptotically Gaussian random variables and thus asymptotically Gaussian themselves. As the ratio of two dependent, asymptotically Gaussian variables, ρ does not, however, have a Gaussian distribution. To derive a parameter distribution, we randomly sample the regression coefficients displayed in table B1 from a Multivariate Gaussian distribution based on their variance-covariance matrix and compute our persistence estimate for each of them. We then use this empirical distribution of the persistence parameter ($N = 1 \times 10^{06}$) for Monte Carlo simulations in PAGE.

While we choose a model with only one lag because of the aforementioned bias-variance tradeoff, it is important to note that including a second lag would strongly reduce a point estimate to 27.8%. A model with four lags even suggests a persistence of only 10.3%. Such lower values might be explained by two effects. Either the economy takes several years after a temperature shock to rebound, implying that our persistence estimate has an upward bias, or the reduced persistence only mirrors the additional noise introduced by further lags. Confidence intervals in table B1 show that with each additional lag, the estimate's distribution shifts towards zero and widens considerably. Including a second lag would extend the 90% confidence interval for ρ to -41%, implying that current climate damages could push the economy to a trajectory of considerably increased growth in the longrun, which seems at odds with the literature on climate change impacts. However, there is, as of yet, no definitive answer as to how many lags one should include. Therefore, we explore the robustness of our approach by adopting another methodology in the following section.

B.4. Estimating persistence based on low-pass filtering

Given the uncertainties outlined in the previous section, we explore the results under a different methodological approach to estimate persistence following Bastien-Olvera and Moore (2021). Their approach, similar to Burke *et al* (2015), regresses GDP per capita growth on temperature and precipitation, but it also applies a Butterworth low-pass filter to the climate variables. By doing this, the authors argue that the estimated impact on economic growth is identified only via long-term temperature variation. This leads to near-zero estimates if the temperature-based damages to GDP are in fact non-persistent. Filtering

Table B1. Results for the baseline regression model by Burke *et al* (2015) for various numbers of temperature lags. Each regression model further contains precipitation, country, and year fixed effects as well as country-specific time trends. Following Burke *et al* (2015), the regression model containing k temperature lags also features k precipitation lags. Here we only report the coefficients for temperature variables that factor into our estimates of damage persistence.

	(1) GDPpc Growth	(2) GDPpc Growth	(3) GDPpc Growth	(4) GDPpc Growth	(5) GDPpc Growth	(6) GDPpc Growth
Temperature	0.0127***	0.0136***	0.0106**	0.00 949**	0.00 933*	0.00 920*
	(3.36)	(3.64)	(3.00)	(2.65)	(2.49)	(2.50)
Temperature squared	−0.000 487***	−0.000 517***	−0.000 456***	−0.000 441***	−0.000 446***	−0.000 459***
	(−4.11)	(−4.33)	(−3.97)	(−3.75)	(−3.62)	(−3.87)
L.Temperature		−0.00 674	−0.00 413	−0.00 549	−0.00 578	−0.00 459
		(−1.56)	(−1.10)	(−1.35)	(−1.43)	(−1.36)
L2.Temperature			−0.00 613	−0.00 638	−0.00 681	−0.00 698
			(−1.63)	(−1.76)	(−1.86)	(−1.95)
L3.Temperature				−0.00 143	−0.000 885	−0.000 993
				(−0.57)	(−0.31)	(−0.38)
L4.Temperature					−0.00 111	−0.00 214
					(−0.42)	(−0.82)
L5.Temperature						0.00 176
						(0.37)
L.Temperature squared		0.000 244*	0.000 206	0.000 240	0.000 245	0.000 228*
		(2.01)	(1.81)	(1.95)	(1.97)	(2.03)
L2.Temperature squared			0.000 123	0.000 126	0.000 133	0.000 146
			(1.14)	(1.22)	(1.28)	(1.43)
L3.Temperature squared				−0.0000 509	−0.0000 779	−0.0000 882
				(−0.59)	(−0.78)	(−0.92)
L4.Temperature squared					0.000 101	0.000 143
					(1.01)	(1.35)
L5.Temperature squared						−0.0000 658
						(−0.43)
Resulting ρ	100%	52.81%	27.82%	28.36%	10.25%	20.81%
5th Monte Carlo percentile	—	0.55%	−73.40%	−101.57%	−143.72%	−94.44%
95th Monte Carlo percentile	—	91.34%	87.77%	106.52%	94.79%	93.10%
N	6584	6519	6398	6277	6155	6031
bic	−19 806.5	−19 677.9	−19 377.4	−19 125.8	−18 744.0	−18 400.4
ll	10 127.4	10 080.4	9942.9	9829.6	9655.6	9500.5

t statistics in parentheses. Standard errors are clustered at the country level.
* $p < 0.05$, ** $p < 0.01$, *** $p < 0.001$.

out high frequencies in temperature and precipitation is statistically beneficial because it does not require additional lag coefficients to be estimated and is therefore less susceptible to noise and multicollinearity if longer time horizons are considered. Therefore, Bastien-Olvera and Moore suggest comparing the estimated marginal impacts for different minimum periodicities to explore if growth impacts of temperature shocks intensify, remain constant, or converge over time.

To derive an estimate of persistence which we can compare with our results, we apply such a low-pass filter to the temperature and precipitation observations in the data by Burke *et al* (2015) for a minimum periodicity of 3, 5, and 10 years, respectively. Following Bastien-Olvera and Moore (2021), we discard countries with less than twice the minimum periodicity $(2 \times 10 = 20)$ of subsequent temperature/precipitation observations for the filtering to work. This reduces the overall number of country-year records in the data only slightly, from 6584 to 6535. Figure B6 illustrates the effect of the low-pass filter for selected countries that are closely aligned with the model regions of PAGE-ICE. We then regress GDP per capita growth on the low-pass filtered climate variables using the main specification by Burke *et al* (2015) and, similar to the lag-based procedure, calculate the implied persistence for the 3 year, 5 year and 10 year

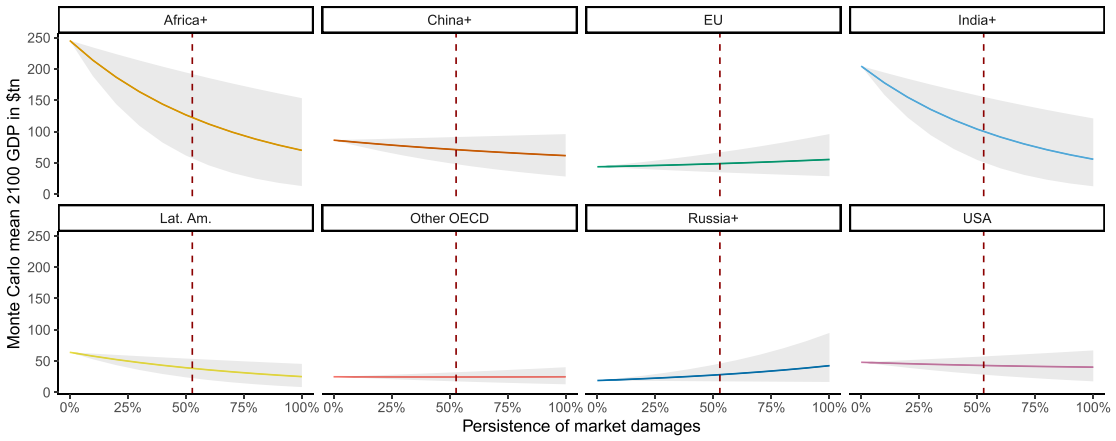

(a) GDP in 2100 for ρ specifications

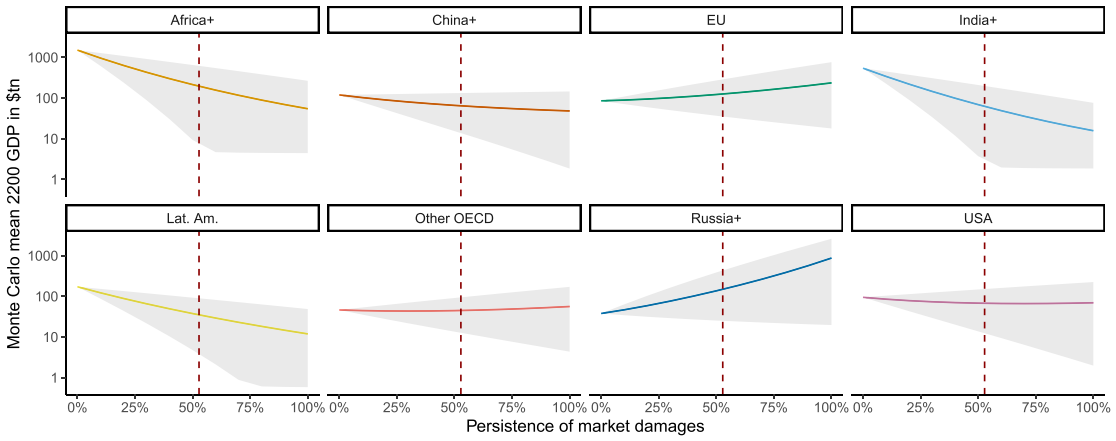

(b) GDP in 2200 for ρ specifications

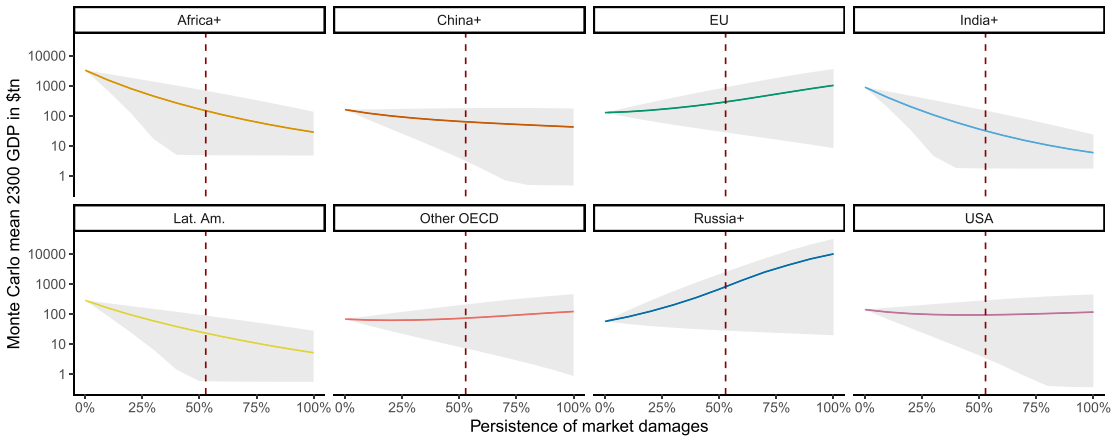

(c) GDP in 2300 for ρ specifications

Figure B5. The effects of the damage persistence parameter ρ on regional GDP levels for different model years for SSP2-4.5 runs. Lines represent the Monte Carlo mean values, while the shaded areas represent the 5th–95th percentile.

filter by dividing the asymptotic marginal impact of the respective regression by the marginal impact of the model without filtering. Note that as this involves comparing the estimates returned by two different regression models (based on either unfiltered or filtered climate variables) the empirical persistence distribution cannot be derived from the variance-covariance matrix of a single regression. To overcome this, we draw with replacement from country clusters to create 5000 bootstrap samples following Burke *et al*

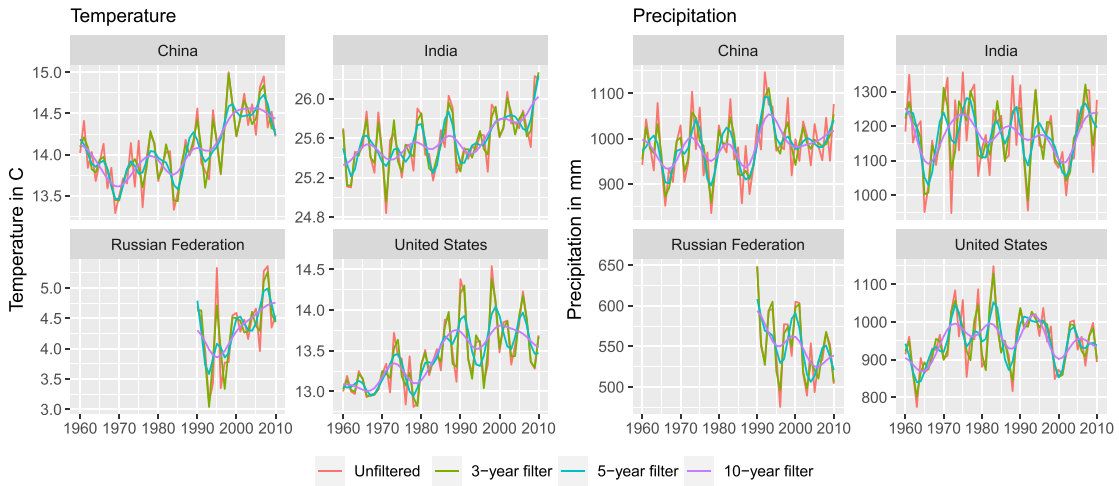

Figure B6. Illustrates effect of a 3, 5, or 10 year low-pass Butterworth filter on temperature and precipitation for selected countries in the data by Burke *et al* (2015).

(2015) and estimate the implied persistence for each bootstrap sample. The results of the regression models for different filter settings and the resulting persistence distribution are displayed in table B2, where the resulting persistence ρ for each filter period is calculated as the asymptotic marginal impact of temperature in the respective column, divided by the asymptotic marginal impact according to the coefficients in column (1).

Table B2 shows that similar to the results under the lag-based approach used in this manuscript, the implied persistence ρ decreases and confidence intervals (or technically, the interval between bootstrap percentiles) widen. For the 3 year filter, the point estimate for ρ is 89.00% which reduces to 52.72% for the 10 year filter. Still, for the 5 year filter, the coefficients for linear and squared temperature remain statistically significant at the 10% level (since the respective t-statistics exceed 1.7). With 9.36%, the 5th bootstrap percentile is well above zero and only 3.6% of the 5000 bootstrap samples yield a non-positive estimate for persistence. For the 10 year filter, temperature coefficients are not significantly different from zero and the 90% bootstrap interval ranges from −60.29% to 118.25%. The point estimate happens to be relatively close to the 52.81% based on the first temperature lag we have used in model runs (see previous section). This exploration indicates that for the data used in this study, the newly proposed method (considering longer time horizons for persistence via low-pass filtering climate variables) does not produce results that show substantially different damage persistence behaviour from the insights in our main approach (assessing persistence via lag coefficients).

We also explore how an empirical persistence distribution based on low-pass filtering would affect our findings with respect to the $SCCO_2$. To this end, we use the bootstrap distribution of ρ by comparing the marginal impacts of unfiltered and 5 year filtered temperature, for which temperature coefficients remain statistically significant at the 10% level. The low-pass filtering approach yields higher persistence levels and hence higher damages. However, as figure B7 illustrates, the Monte Carlo mean $SCCO_2$ decreases from \$3372 under the lag-based approach to \$3025 for the distribution using low-pass filtering. The primary reason is that the latter on average yields a higher persistence and hence more Monte Carlo runs in which the maximum amount of damages in the model is reached and the $SCCO_2$ becomes zero. More specifically, the share of Monte Carlo runs with a $SCCO_2$ of zero increases from 62% under the lag-based approach to 69% based on low-pass filtering.

B.5. Regional heterogeneity of damage persistence

In our main model, we implement persistence as a global parameter. We recognize that this is a very strong assumption and does not represent heterogeneity across climate zones or income levels. Research on adaptive capacity research has identified many potential barriers to adaptation, which differ strongly depending on the context (Eisenack *et al* 2014). Thus, one might expect differences in the persistence parameter across countries (and thus across PAGE-ICE regions) due to, for instance, income differences or other social and geographic contexts.

To explore the empirical evidence for this, we repeat the persistence estimation procedure for two groups of countries: rich and poor countries. We follow Burke *et al* (2015) by assigning each country in the data to one of two subsamples based on whether its 1980 GDP per capita, with conversion based on

Table B2. Regressing GDP per capita growth in the Burke *et al* (2015) data on low-pass filtered climate variables.

	(1) Unfiltered	(2) 3 year filter	(3) 5 year filter	(4) 10 year filter
Temperature	0.012 933***	0.012 211**	0.009 065	0.009 761
	(3.41)	(2.79)	(1.71)	(0.90)
Temperature^2	−0.000 490***	−0.000 436**	−0.000 299	−0.000 258
	(−4.11)	(−3.24)	(−1.88)	(−0.95)
Resulting ρ	100.00%	89.00%	61.09%	52.72%
5th percentile	—	69.33%	9.36%	−60.29%
95th percentile	—	102.40%	91.38%	118.25%
N	6535	6535	6535	6535
BIC	−19 634.1	−19 632.5	−19 620.8	−19 615.5
ll	10 045.5	10 040.3	10 034.4	10 031.8

t statistics in parentheses. Standard errors are clustered at the country level.
Percentiles are estimated via 5000 cluster bootstrap samples.
* $p < 0.05$, ** $p < 0.01$, *** $p < 0.001$.
Author's calculations based on the data provided by Burke *et al* (2015).

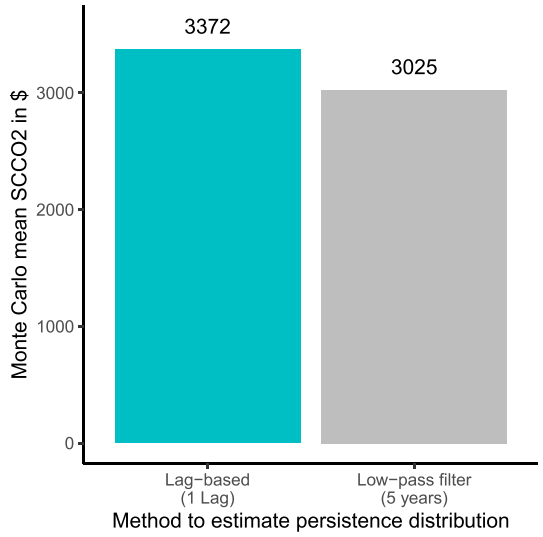

Figure B7. Mean $SCCO_2$ based on 50 000 Monte Carlo under different methodologies to estimate the persistence distribution for SSP2-4.5. The blue bar marks our default setting.

purchasing power parity (PPP), was above or below the sample median. We then repeat our main lag-based approach to estimate persistence separately for each of these income-based subsamples and display the results in tables B3 and B4.

Since subsampling approximately halves the sample size, overall statistical power is diminished. Standard errors increase considerably for all numbers of lags under consideration. In particular, the coefficients on the first temperature lag are no longer statistically significant for either of the two subsamples. For both income groups, the signs of the 1st lag is opposite to the sign of the immediate temperature impact, suggesting less than full persistence. The point estimates for the persistence parameter ρ in the poorer and richer subsample are 42.48% and 61.97%, respectively. When two or more lags are used, the persistence estimate for the below-median sample becomes negative while the estimate for the richer subsample remains positive ,but much closer to zero. However, Monte Carlo experiments show that estimates for ρ vary considerably and even when using one lag only, the 5th Monte Carlo percentiles ranges below zero for the lower- and higher-income subsamples (at −146.71% and −95.71%, respectively). Regression tables B3 and B4 thus remain largely inconclusive with respect to whether spatially heterogeneity should be implemented in the ρ parameter. Therefore, we conclude that while there might very well be regional differences in the actual persistence of climate damages, we do not find clear evidence in this data set for applying heterogeneous persistence under the lag-based approach in our model.

To explore the possibilities of regional heterogeneity in persistence further, we also apply the low-pass filtering approach outlined above separately to the income-based subsample of the Burke *et al* (2015) data and display the results in tables B5 and B6. Note that we remove countries with less than 20 temperature-precipitation observations for the low-pass filtering to work which reduces the initial sample size slightly. Similar to the lag-based approach, confidence intervals for the two subsamples are considerably wider compared to the full sample in table B2, reducing t statistics for the individual temperature coefficients and increasing the

Table B3. Results for the baseline regression model by Burke *et al* (2015) for countries with GDPpc *below* the median and various numbers of temperature lags. Each regression model further contains precipitation, country and year fixed effects as well as country-specific time trends. Following Burke *et al* (2015), the regression model containing k temperature lags also features k precipitation lags. Here we only report the coefficients for temperature variables that factor into our estimates of damage persistence.

	(1) GDPpc Growth	(2) GDPpc Growth	(3) GDPpc Growth	(4) GDPpc Growth	(5) GDPpc Growth	(6) GDPpc Growth
Temperature	0.0236	0.0246	0.0096	0.0048	0.0029	−0.0040
	(1.34)	(1.48)	(0.60)	(0.32)	(0.19)	(−0.28)
Temperature squared	−0.0007	−0.0007*	−0.0004	−0.0003	−0.0003	−0.0002
	(−1.89)	(−2.08)	(−1.25)	(−0.99)	(−0.87)	(−0.51)
L.Temperature		−0.0150	−0.0035	−0.0049	−0.0043	0.0009
		(−0.88)	(−0.33)	(−0.46)	(−0.43)	(0.10)
L2.Temperature			−0.0165	−0.0180	−0.0206	−0.0240
			(−0.95)	(−1.01)	(−1.10)	(−1.32)
L3.Temperature				0.0061	0.0049	0.0046
				(0.65)	(0.44)	(0.44)
L4.Temperature					0.0021	−0.0020
					(0.17)	(−0.18)
L5.Temperature						0.0083
						(1.18)
L.Temperature squared		0.0004	0.0002	0.0003	0.0002	0.0001
		(1.18)	(0.93)	(1.09)	(1.06)	(0.69)
L2.Temperature squared			0.0003	0.0003	0.0004	0.0004
			(0.77)	(0.82)	(0.94)	(1.16)
L3.Temperature squared				−0.0002	−0.0002	−0.0002
				(−0.85)	(−0.81)	(−0.83)
L4.Temperature squared					0.0001	0.0002
					(0.31)	(0.77)
L5.Temperature squared						−0.0003
						(−1.59)
Resulting ρ	100.00%	42.48%	−16.29%	−15.89%	−69.83%	−94.29%
5th Monte Carlo percentile	—	−146.71%	−894.45%	−923.95%	−1246.10%	−1081.44%
95th Monte Carlo percentile	—	135.33%	905.03%	1022.92%	1345.78%	1332.94%
N	3429	3391	3332	3273	3214	3154
bic	−9681.9	−9564.9	−9420.3	−9264.0	−9086.2	−8911.6
ll	5048.5	5006.0	4945.4	4882.9	4805.6	4729.7

t statistics in parentheses.

* $p < 0.05$, ** $p < 0.01$, *** $p < 0.001$.

Author's calculations based on the data provided by Burke *et al* (2015).

uncertainty about the persistence level ρ. However, we see different behavior in filters with larger periodicity. Point estimates for the higher-income countries decrease for a larger filter periodicity (from 69.76% for the 3 year filter to −2.91% for the 10 year filter in table B6) and even for the 3 year filter, the bootstrap interval is almost symmetric around zero, indicating low evidence for persistence. In contrast, the point estimates for the lower-income subsample range between 73.29% and 112.45% for different filter periods (see table B5). Notably, the poorer subset's 95% bootstrap interval does not include zero for the 3 year filter and even for the 5 year filter, 88.8% of the 5000 bootstrap samples yield a persistence estimate above zero. Therefore, we conclude that unlike the lag-based approach, estimating persistence via low-pass filters provides some suggestive evidence that poorer regions might be more vulnerable to persistent growth impacts of temperature shocks.

To illustrate the implications of regional differentiation for the $SCCO_2$, we carry out an additional robustness check by applying our main persistence distribution (derived via temperature lag coefficients) only to the four PAGE-ICE model regions with the lowest initial GDP per capita in the 2015 base year,

Table B4. Results for the baseline regression model by Burke *et al* (2015) for countries with GDPpc *above* the median and various numbers of temperature lags. Each regression model further contains precipitation, country and year fixed effects as well as country-specific time trends. Following Burke *et al* (2015), the regression model containing k temperature lags also features k precipitation lags. Here we only report the coefficients for temperature variables that factor into our estimates of damage persistence.

	(1) GDPpc Growth	(2) GDPpc Growth	(3) GDPpc Growth	(4) GDPpc Growth	(5) GDPpc Growth	(6) GDPpc Growth
Temperature	0.0085*	0.0092*	0.0084*	0.0077	0.0074	0.0082*
	(2.22)	(2.42)	(2.22)	(1.97)	(1.77)	(2.04)
Temperature squared	−0.0003*	−0.0004*	−0.0004*	−0.0004*	−0.0004*	−0.0004*
	(−2.16)	(−2.24)	(−2.23)	(−2.18)	(−2.11)	(−2.43)
L.Temperature		−0.0044	−0.0032	−0.0045	−0.0053	−0.0051
		(−0.89)	(−0.66)	(−0.87)	(−0.98)	(−1.16)
L2.Temperature			−0.0067	−0.0065	−0.0062	−0.0069*
			(−1.83)	(−1.85)	(−1.80)	(−2.06)
L3.Temperature				−0.0024	−0.0026	−0.0018
				(−0.82)	(−0.79)	(−0.58)
L4.Temperature					−0.0006	−0.0008
					(−0.23)	(−0.27)
L5.Temperature						−0.0015
						(−0.27)
L.Temperature squared		0.0001	0.0001	0.0002	0.0002	0.0002
		(0.82)	(0.69)	(0.84)	(0.94)	(1.07)
L2.Temperature squared			0.0002	0.0002	0.0002	0.0002
			(1.69)	(1.60)	(1.40)	(1.73)
L3.Temperature squared				−0.0001	−0.0000	−0.0001
				(−0.38)	(−0.13)	(−0.44)
L4.Temperature squared					−0.0000	0.0000
					(−0.22)	(0.00)
L5.Temperature squared						0.0001
						(0.36)
Resulting ρ	100.00%	61.97%	1.21%	12.90%	18.08%	0.22%
5th Monte Carlo percentile	—	−95.71%	−323.86%	−391.63%	−370.90%	−229.34%
95th Monte Carlo percentile	—	147.38%	117.18%	148.72%	159.32%	109.67%
N	3155	3128	3066	3004	2941	2877
bic	−9923.1	−9894.5	−9721.7	−9606.1	−9396.5	−9228.0
ll	5167.0	5168.6	5093.7	5047.3	4953.8	4880.8

t statistics in parentheses.

* $p < 0.05$, ** $p < 0.01$, *** $p < 0.001$.

Author's calculations based on the data provided by Burke *et al* (2015).

namely China+, India+, Africa+ and Latin America. Simultaneously we thus assume for this run that the EU, Russia+, USA and Other OECD regions do not face alterations from their scenario-based long-term growth trajectory, though they will still suffer from contemporary market damages. Figure B8 illustrates the relatively small effect of this change, in part because Global North regions can see opposing effects of temperature increases. Due to generally slightly lower damages, the overall mean $SCCO_2$ would be slightly higher because fewer Monte Carlo runs reach the maximum amount of overall damages in the model. The share of runs with an $SCCO_2$ of zero decreases from 62.3% to 61.7%. Overall, our findings are primarily driven by persistence in regions with lower GDP per capita and do not change strongly if richer regions were less vulnerable to damage persistence (or much quicker to adapt).

Table B5. Regressing GDP per capita growth in the Burke *et al* (2015) data on low-pass filtered climate variables—*below* GDPpc median.

	(1) Unfiltered	(2) 3 year filter	(3) 5 year filter	(4) 10 year filter
Temperature	0.025 169	0.031 177	0.019 792	0.034 540
	(1.43)	(1.75)	(0.75)	(0.60)
Temperature^2	−0.000 749	−0.000 842*	−0.000 549	−0.000 806
	(−1.97)	(−2.19)	(−0.98)	(−0.67)
Resulting ρ	100.00%	112.45%	73.29%	107.71%
5th percentile	—	84.12%	−62.78%	−296.33%
95th percentile	—	164.32%	155.72%	340.61%
N	3391	3391	3391	3391
BIC	−9556.7	−9552.6	−9542.3	−9541.1
ll	4985.6	4983.6	4978.4	4977.8

t statistics in parentheses. Standard errors are clustered at the country level.
Percentiles are estimated via 5000 cluster bootstrap samples.
* $p < 0.05$, ** $p < 0.01$, *** $p < 0.001$.
Author's calculations based on the data provided by Burke *et al* (2015).

Table B6. Regressing GDP per capita growth in the Burke *et al* (2015) data on low-pass filtered climate variables—*above* GDPpc median.

	(1) Unfiltered	(2) 3 year filter	(3) 5 year filter	(4) 10 year filter
Temperature	0.008 412*	0.006 184	0.004 519	0.000 073
	(2.20)	(1.30)	(0.73)	(0.01)
Temperature^2	−0.000 330*	−0.000 230	−0.000 135	0.000 010
	(−2.13)	(−1.23)	(−0.58)	(0.03)
Resulting ρ	100.00%	69.76%	40.96%	−2.91%
5th percentile	—	−70.72%	−248.19%	−631.26%
95th percentile	—	97.68%	106.27%	117.74%
N	3144	3144	3144	3144
BIC	−9883.0	−9879.2	−9876.6	−9875.4
ll	5146.8	5145.0	5143.7	5143.1

t statistics in parentheses. Standard errors are clustered at the country level.
Percentiles are estimated via 5000 cluster bootstrap samples.
* $p < 0.05$, ** $p < 0.01$, *** $p < 0.001$.
Author's calculations based on the data provided by Burke *et al* (2015).

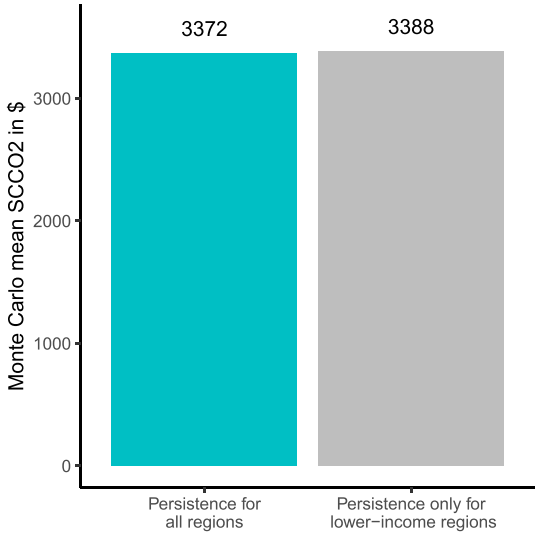

Figure B8. Mean $SCCO_2$ based on 50 000 Monte Carlo using persistence as a global parameter or limiting it to lower-income regions for SSP2-4.5. The blue bar marks our default setting.

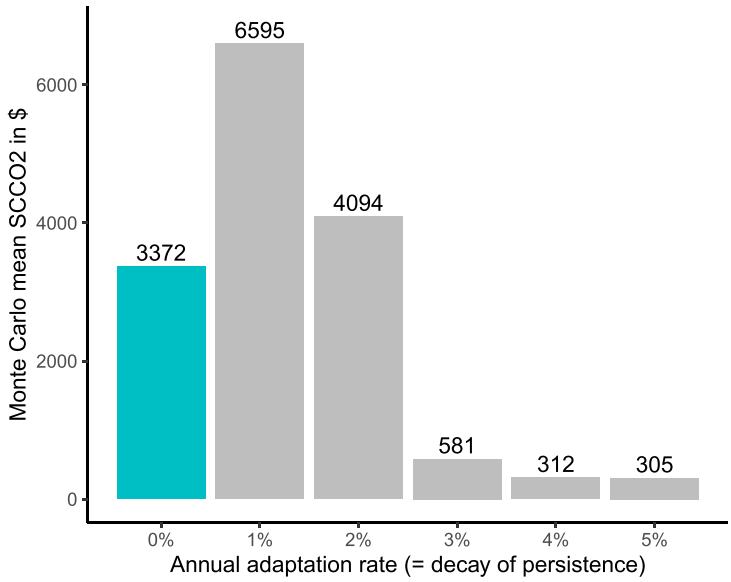

Figure B9. Mean $SCCO_2$ based on 50 000 Monte Carlo under different annual decay rates of damage persistence for SSP2-4.5. The blue bar marks our default setting of zero decay, (i.e. damage persistence remains constant over time).

B.6. Adaptation to damage persistence applied to the empirical distribution

By using historical data to calibrate our estimate of damage persistence and extrapolating it into the distant future, we implicitly assume (in figure 3) that future persistence will equal the persistence levels observed over the past decades, consistent with Burke *et al* (2015). It is, however, possible that the increased economic damages due to climate change will trigger a rise in adaptation efforts which might not only reduce current damages, but also limit the vulnerability of capital stocks (both physical and human) to climate change. If this is the case, then our assumption of extrapolating previous persistence levels might turn out to be too pessimistic. In the absence of empirical evidence or mechanistic understanding of how temperature damages might persist in future scenarios, we explore the theoretical possibility that damage persistence (ρ) decays exponentially over time following a similar approach adopted by Moore and Diaz (2015) for the DICE CB-IAM. Figure B9 illustrates the impacts of varying decay rates on our $SCCO_2$ estimate under SSP2-4.5.

An annual decay of 3% or higher greatly reduces the estimated marginal damages of CO_2 emissions, especially later in the model horizon for the regions with the highest temperatures, when the highest climate change-induced economic damages are reached, but the degree of persistence has decayed to low levels. If damage persistence decreases by 4%–5% per year, the $SCCO_2$ equals \$305–312 which is virtually identical to the $SCCO_2$ for the default PAGE-ICE model with no persistence.

A decay rate of 1% or 2% counterintuitively increases the $SCCO_2$ compared to our default with zero decay from \$3372 to \$6595 or \$4094 respectively, because of interactions with the cap for overall damages in PAGE-ICE. With low decay rates, fewer Monte Carlo simulations reach the cap, which decreases the share of model runs with a $SCCO_2$ of zero and thus increases the Monte Carlo mean.

Appendix C. Temperature variability models

C.1. Historical temperature analysis

The historical temperature dataset used is described in Ilyas *et al* (2017), which is a variant of HadCRUT4 (Morice *et al* 2012) and is available at https://oasishub.co/dataset/global-monthly-temperature-ensemble-1850-to-2016. A multi-resolution lattice kriging approach was used to estimate the uncertainties related to limited spatial coverage in HadCRUT4. 10 000 ensemble members together express probabilistic gridded temperatures.

The current body of literature does not conclusively answer whether interannual variability is increasing globally, but observation-based studies appear to indicate little change in global annual mean temperature variability (Alexander and Perkins 2013, Huntingford *et al* 2013). After Huntingford *et al* (2013), we compute interannual temperature variability in our dataset as the long-term average of the 11 year standard deviations after detrending the annual temperature anomaly data using a local 11 year running mean. Figure C1 shows the interannual variability for used period 1986–2015, compared to pre-1986 levels. We identify no clear overall positive or negative trend in interannual variabiility from

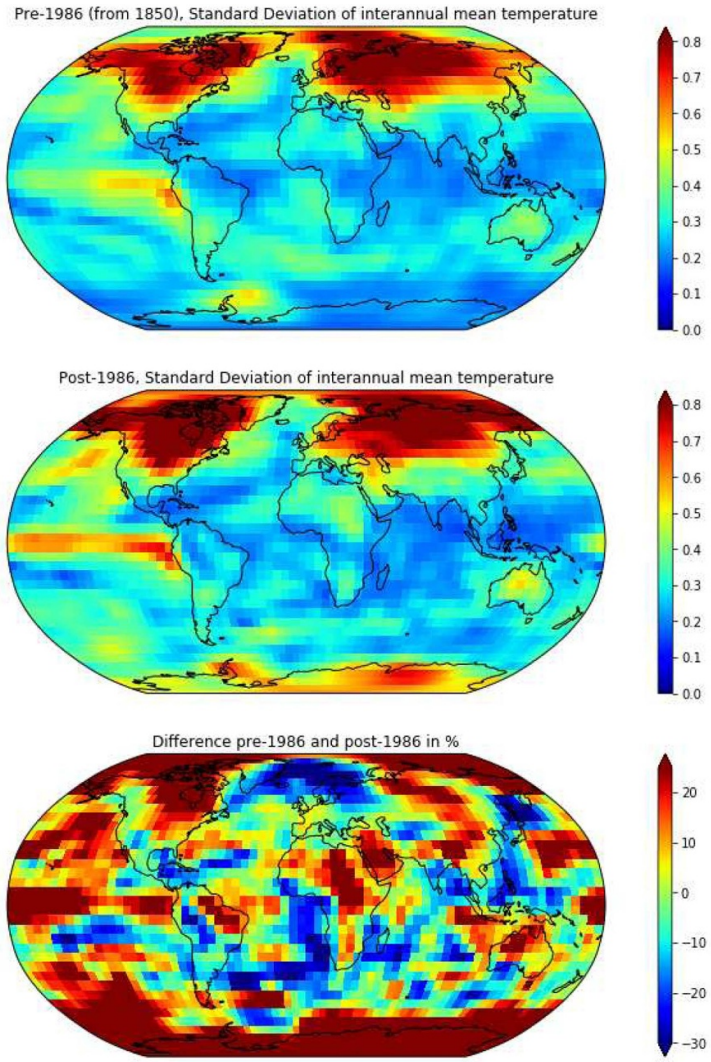

Figure C1. Local interannual mean temperature variability. Annual standard deviations are calculated over 11 year detrended periods. Local means of this standard deviation are plotted for the period on the record before 1986 and after 1986. The local change between the two time periods is shown in percentages.

the Ilyas *et al* (2017) dataset. Contrary to Huntingford *et al* (2013), we find strongly positive changes over the tropics, especially over Amazonia, whilst we see little increases in variability over Europe. Some of this difference probably arises from the longer records in our analysis, but the more rigorous treatment of uncertainties during interpolation used in this study may be another minor underlying difference (Beguería *et al* 2016). Nonetheless, even for a longer time series analysis, we do not find global or PAGE-ICE region-specific evidence that justifies increasing or decreasing temperature variability with rising global temperatures in simulations.

To find the level of interannual variability per region, we apply a land-sea mask to the coarse HadCRUT4 grid, followed by multiplying with the cosine of the latitude. Consequently, annual mean temperatures are calculated for the PAGE-ICE regions by spatial aggregation. A 30-year running window is used for linear detrending to remove the global warming signal, before the standard deviation is calculated over that 30 year window, following, for example, Huntingford *et al* (2013). We use the results for the period 1986–2015, which are found in table C1. The medians of the ensemble, which are provided separately, are used in the main model specification.

C.2. Autoregressive temperature model

Temperatures exhibit a considerable degree of autocorrelation across years. Table C2 displays regression models of temperature, showing autocorrelation levels of over 0.3. These are computed using the regional temperature data summarized in table C1. We use column (5) from table C2 as a basis for decomposing annual temperature variability into autocorrelation, smooth trends, and random variability. The smooth trend, which is represented in the regression model with locally estimated scatterplot smoothing (LOESS), is equivalent to the underlying climatic temperature computed in PAGE (PT_g). Figure C2 shows several realizations of the autoregressive model, which roughly captures both

Table C1. Standard deviations (in °C) of annual spatially aggregated mean temperature variability based on of the linearly detrended temperatures for 1986–2015, with uncertainties (1 standard deviation) based on the full 10 000 member ensemble.

	Variability of median local temperatures (Std. Dev. [°C])	Variability of mean local temperatures (Std. Dev. [°C])	Uncertainty in observations (Std. Dev. [°C])
EU	0.415	0.352	0.0191
Russia+	0.440	0.397	0.0302
USA	0.364	0.392	0.0304
China+	0.265	0.260	0.0594
India+	0.201	0.200	0.0399
Africa and Middle East	0.196	0.182	0.0502
Latin America	0.154	0.156	0.0542
Other OECD	0.362	0.353	0.0430
Global	0.110	0.113	0.0216

the variability and temporal structure of observed temperatures.

The amount of autoregressivity varies by PAGE region, from 0.012 (Other OECD) to 0.200 (India+) (see table C3). These levels of autoregression are low both because of the inherently greater variability of weather at a local scale and because the contemporaneous global temperature is controlled for. We use the results of column (5) in tables C2 and C3 in a two-step process to add autocorrelated temperatures to PAGE-ICE.

In this new version, we compute the global temperature as

$$RT_{gt} \sim \begin{cases} \mathcal{N}\left(PT_{gt}, \sigma_g\right) & \text{if } t = 1 \\ \mathcal{N}(\alpha_g + \beta_g PT_{gt} + \gamma_g(PT_{gt} - PT_{g,t-1} + RT_{g,t-1}), \sigma_g) & \text{else} \end{cases}$$

where α_g, β_g, and γ_g are the constant, LOESS, and autoregression terms from model (5) in table C2, and σ_g is the corresponding standard error of the residuals. The $PT_{g,t-1}$ variable is the same as PAGE-ANN. The term $PT_{gt} - PT_{g,t-1}$ removes the lagging of temperatures that would otherwise by observed in RT_{gt} due to the autoregression.

Next, we compute regional temperatures as

$$RTL_{rt} \sim \begin{cases} \mathcal{N}\left(\mathrm{AF}_r RT_{gt}, \sigma_r\right) & \text{if } t = 1 \\ \mathcal{N}\left(\frac{\mathrm{AF}_r}{\beta_r + \gamma_r}\left(\alpha_r + \beta_r RTL_{rt} + \gamma_r(\mathrm{AF}_r(PT_{gt} - PT_{g,t-1}) + RT_{g,t-1})\right), \sigma_g\right) & \end{cases}$$

where AF_r is the PAGE amplification factor. The $\mathrm{AF}_r(PT_{gt} - PT_{g,t-1})$ term is again introduced to remove lagging temperatures. The entire regression-based expression is multiplied by $\frac{\mathrm{AF}_r}{\beta_r + \gamma_r}$ to scale the regional temperatures to approximate the original PAGE results, $\mathrm{AF}_r RT_{gt}$, accounting for any mismatch between the regional temperature dataset and PAGE's regional calibration.

Under this model, we assume that residual temperature variation is uncorrelated across regions, after accounting for GMST and regional auto-regression. Since the regions used in PAGE are chosen for economic coherence, rather than climatological distinctness, we test this assumption by looking at the correlation in model errors across regions from our model.

As shown in figure C3, compared to the correlation across regions in the raw temperatures, controlling for either a smoothed GMST predictor or an auto-regressive term reduces average correlation of the residuals across regions by half. The full model, including both a smooth GMST predictor and

Table C2. Models of annual temperature, accounting for trends and auto-correlation. Columns 1–3 represent different models of the smooth trends behind annual temperatures, using a simple trend (1), CO_2 concentrations (2), and a LOESS of observed GMST (3). Columns (4) and (5) show combinations.

	Dependent variable:				
			$GMST_t$		
	(1)	(2)	(3)	(4)	(5)
Year	0.006^{***}				
	(0.0003)				
$GMST_{t-1}$				0.402^{***}	0.315^{***}
				(0.071)	(0.074)
CO_2 (ppm)		0.010^{***}		0.006^{***}	
		(0.0004)		(0.001)	
LOESS			1.007^{***}		0.693^{***}
			(0.033)		(0.080)
Constant	-10.822^{***}	-2.867^{***}	−0.009	-1.732^{***}	−0.005
	(0.628)	(0.112)	(0.014)	(0.226)	(0.014)
Observations	169	169	169	168	168
R^2	0.652	0.825	0.847	0.853	0.862
Adjusted R^2	0.650	0.824	0.846	0.851	0.860
Residual Std. Error	0.206	0.146	0.136	0.134	0.130

$^{*}p<0.1$; $^{**}p<0.05$; $^{***}p<0.01$.

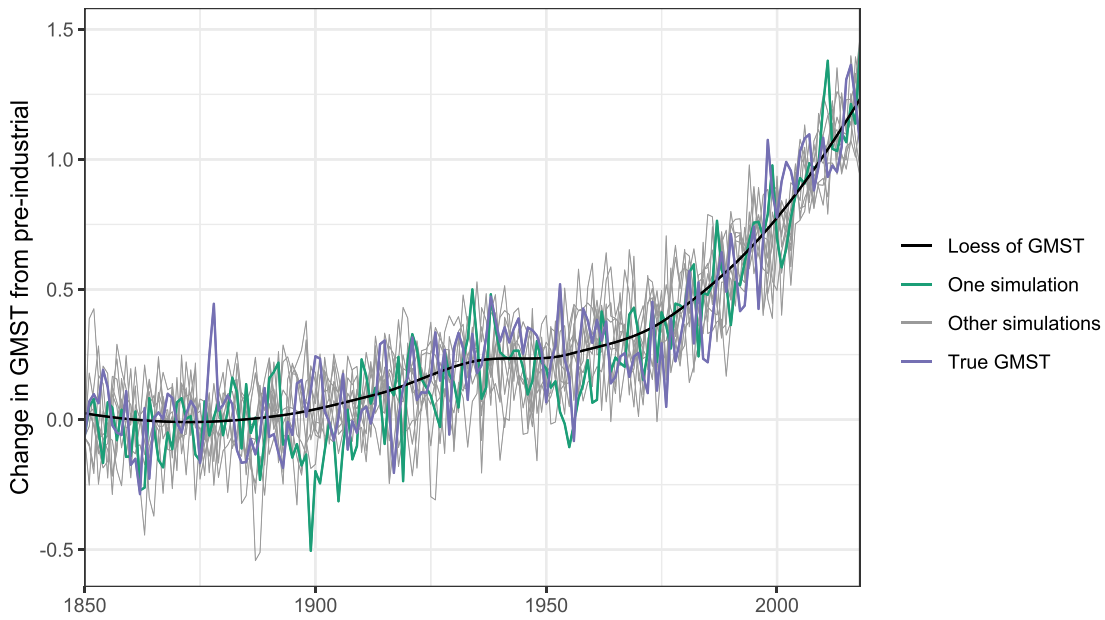

Figure C2. Simulations of the autoregressive temperature model. Several simulations are shown in grey, with one highlighted in green. The observed GMST timeseries is shown in purple, with the LOESS of this in black.

auto-regressive terms, approximately halves the cross-region correlation again, to a median 0.15 correlation. The final variance of these residuals is also reduced, from 0.22 for raw temperatures to 0.04 for the full model.

C.3. Alternative temperature model with independent temperature variability

As an additional result, we explore the effects of a simpler specification of temperature variability that takes into account observational uncertainties. We specify this alternative model without autogression as follows:

$$T_{g,t+1} = \Theta_{gt} + \mathcal{N}(0, \mathcal{N}(\mu_g^2, \Delta_g^2)) \quad \text{(C1}a\text{)}$$

$$T_{g,t+1} = \Theta_{gt} \cdot AF_r + \mathcal{N}(0, \mathcal{N}(\mu_r^2, \Delta_r^2)) \quad \text{(C1}b\text{)}$$

where μ represents the standard deviations on the mean annual temperature for a geographical region, and Δ is the standard deviation capturing the uncertainty in the 10 000 member ensemble. Δ of the two is specified exogenously in the Monte Carlo draw for each run, while μ is randomly drawn every year. The impacts of this alternative model on the $SCCO_2$ are shown in table A4.

Table C3. Regression results of the autoregressive model by region.

	Dependent variable: Reg. Temp$_t$							
	EU	Rus+	USA	Chi+	Ind+	Afr+	Lat	Oth
Reg. Temp$_{t-1}$	0.073	0.060	0.046	0.190***	0.200***	0.123**	0.232***	0.012
	(0.069)	(0.059)	(0.062)	(0.057)	(0.058)	(0.062)	(0.064)	(0.053)
GMST	1.243***	1.766***	1.182***	1.010***	0.709***	0.949***	0.652***	1.604***
	(0.118)	(0.124)	(0.090)	(0.077)	(0.055)	(0.071)	(0.060)	(0.094)
Constant	0.006	0.059	−0.029	−0.008	−0.020	−0.020	−0.005	0.018
	(0.039)	(0.037)	(0.029)	(0.019)	(0.015)	(0.015)	(0.015)	(0.026)
Observations	168	168	168	168	168	168	168	168
R^2	0.583	0.764	0.691	0.831	0.795	0.856	0.785	0.827
Adjusted R^2	0.578	0.761	0.687	0.829	0.792	0.854	0.783	0.825
Residual Std. Error	0.394	0.363	0.288	0.194	0.154	0.154	0.154	0.259

* $p<0.1$; ** $p<0.05$; *** $p<0.01$.

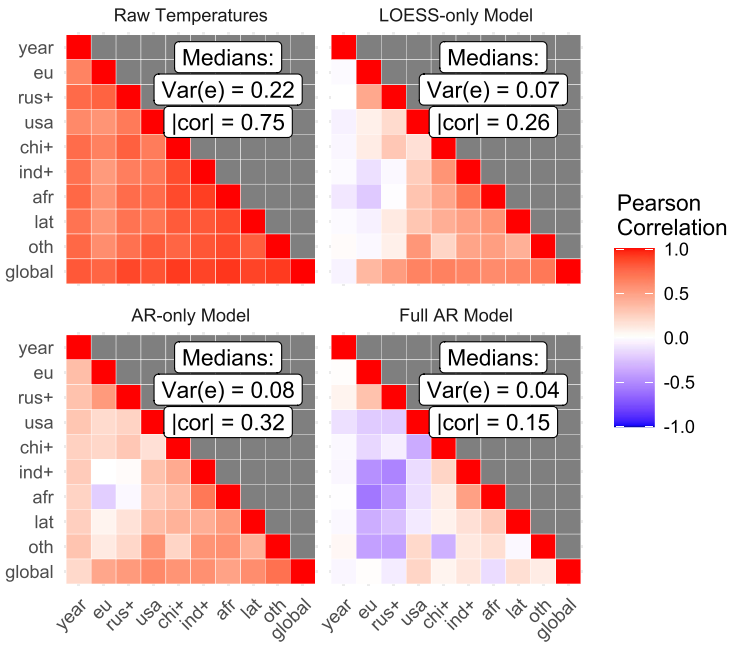

Figure C3. Correlation in the model errors across regions. The four subplots represent different models, within which each row and column describes residuals for a region, or the numerical year ('year'), or the global GMST model ('global'). The cells are colored by the Pearson correlation of these residuals. Each subplot also reports the median variance of the model errors ('Var(e)') across regions, and the median absolute value of the correlation of all off-diagonal correlations ('|cor|'). The 'Raw Temperatures' subplot treats all variation in temperatures as model error; the 'LOESS-only Model' subplot regresses region temperatures on a smoothed GMST; the 'AR-only Model' subplot regressions region temperatures on delayed temperatures; and the 'Full AR Model' includes both regressors.

ORCID iDs

Jarmo S Kikstra https://orcid.org/0000-0001-9405-1228
Paul Waidelich https://orcid.org/0000-0002-5081-776X
James Rising https://orcid.org/0000-0001-8514-4748
Dmitry Yumashev https://orcid.org/0000-0003-1355-2827
Chris M Brierley https://orcid.org/0000-0002-9195-6731

References

Alexander L and Perkins S 2013 Debate heating up over changes in climate variability *Environ. Res. Lett.* **8** 041001
Andrijevic M, Crespo Cuaresma J, Muttarak R and Schleussner C F 2020 Governance in socioeconomic pathways and its role for future adaptive capacity *Nat. Sustain.* **3** 35–41
Anthoff D, Hepburn C and Tol R S 2009a Equity weighting and the marginal damage costs of climate change *Ecol. Econ.* **68** 836–49
Anthoff D, Tol R S and Yohe G W 2009b Risk aversion, time preference and the social cost of carbon *Environ. Res. Lett.* **4** 024002
Bastien-Olvera B and Moore F 2021 Persistent effect of temperature on GDP identified from lower frequency temperature variability (available at: https://doi.org/10.21203/rs.3.rs-601512/v1)
Beguería S, Vicente-Serrano S M, Tomás-Burguera M and Maneta M 2016 Bias in the variance of gridded data sets leads to misleading conclusions about changes in climate variability *Int. J. Climatol.* **36** 3413–22
Burke M *et al* 2016 Opportunities for advances in climate change economics *Science* **352** 292–3
Burke M and Emerick K 2016 Adaptation to climate change: evidence from US agriculture *Am. Econ. J.: Econ. Policy* **8** 106–40
Burke M, Hsiang S M and Miguel E 2015 Global non-linear effect of temperature on economic production *Nature* **527** 235–9
Byers E *et al* 2018 Global exposure and vulnerability to multi-sector development and climate change hotspots *Environ. Res. Lett.* **13** 055012
Cai Y, Lenton T M and Lontzek T S 2016 Risk of multiple interacting tipping points should encourage rapid CO_2 emission reduction *Nat. Clim. Change* **6** 520–5
Calvin K, Bond-Lamberty B, Jones A, Shi X, Di Vittorio A and Thornton P 2019 Characteristics of human-climate feedbacks differ at different radiative forcing levels *Glob. Planet. Change* **180** 126–35
Carleton T A *et al* 2020 Valuing the global mortality consequences of climate change accounting for adaptation costs and benefits *Working Paper* 27599 (National Bureau of Economic Research) (available at: www.nber.org/papers/w27599)
Carleton T and Greenstone M 2021 Updating the United States Government's social cost of carbon *SSRN Electron. J.* **2021-04** 1–49
Dell M, Jones B F and Olken B A 2012 Temperature shocks and economic growth: evidence from the last half century *Am. Econ. J.: Macroecon.* **4** 66–95
Diaz D and Moore F 2017 Quantifying the economic risks of climate change *Nat. Clim. Change* **7** 774–82
Dietz S 2011 High impact, low probability? An empirical analysis of risk in the economics of climate change *Clim. Change* **108** 519–41
Dietz S and Stern N 2015 Endogenous growth, convexity of damage and climate risk: how Nordhaus' framework supports deep cuts in carbon emissions *Econ. J.* **125** 574–620

Dolphin G, Pollitt M G and Newbery D M 2020 The political economy of carbon pricing: a panel analysis *Oxf. Econ. Pap.* **72** 472–500

Eisenack K, Moser S C, Hoffmann E, Klein R J, Oberlack C, Pechan A, Rotter M and Termeer C J 2014 Explaining and overcoming barriers to climate change adaptation *Nat. Clim. Change* **4** 867–72

Estrada F, Tol R S and Gay-García C 2015 The persistence of shocks in GDP and the estimation of the potential economic costs of climate change *Environ. Modelling Softw.* **69** 155–65

Fankhauser S and Tol R S 2005 On climate change and economic growth *Resour. Energy Econ.* **27** 1–17

Field C B *et al* 2012 *Managing the Risks of Extreme Events and Disasters to Advance Climate Change Adaptation: Special Report of the Intergovernmental Panel on Climate Change*

Glanemann N, Willner S N and Levermann A 2020 Paris climate agreement passes the cost-benefit test *Nat. Commun.* **11** 110

Hallegatte S and Dumas P 2009 Can natural disasters have positive consequences? Investigating the role of embodied technical change *Ecol. Econ.* **68** 777–86

Havranek T, Irsova Z, Janda K and Zilberman D 2015 Selective reporting and the social cost of carbon *Energy Econ.* **51** 394–406

Hope C 2013 Critical issues for the calculation of the social cost of CO2: why the estimates from PAGE09 are higher than those from PAGE2002 *Clim. Change* **117** 531–43

Hope C 2015 The $10 trillion value of better information about the transient climate response *Phil. Trans. R. Soc.* A **373** 20140429

Howard P H and Sterner T 2017 Few and not so far between: a meta-analysis of climate damage estimates *Environ. Resour. Econ.* **68** 197–225

Hsiang S M 2010 Temperatures and cyclones strongly associated with economic production in the Caribbean and Central America *Proc. Natl Acad. Sci. USA* **107** 15367–72

Huntingford C, Jones P D, Livina V N, Lenton T M and Cox P M 2013 No increase in global temperature variability despite changing regional patterns *Nature* **500** 327–30

Ilyas M, Brierley C M and Guillas S 2017 Uncertainty in regional temperatures inferred from sparse global observations: application to a probabilistic classification of El Niño *Geophys. Res. Lett.* **44** 9068–74

Interagency Working Group 2013 Technical update on the social cost of carbon for regulatory impact analysis-under executive order 12866 *Technical Report*

IPCC 2018 Special report on global warming of 1.5 °C *Technical Report*

Jones M R, Fowler H J, Kilsby C G and Blenkinsop S 2013 An assessment of changes in seasonal and annual extreme rainfall in the UK between 1961 and 2009 *Int. J. Climatol.* **33** 1178–94

Kahn M E, Mohaddes K, Ng R N, Pesaran M H, Raissi M and Yang J-C 2019 Long-term macroeconomic effects of climate change: a cross-country analysis *Technical Report* (National Bureau of Economic Research)

Kalkuhl M and Wenz L 2020 The impact of climate conditions on economic production. Evidence from a global panel of regions *J. Environ. Econ. Manage.* **103** 102360

Kotz M, Wenz L, Stechemesser A, Kalkuhl M and Levermann A 2021 Day-to-day temperature variability reduces economic growth *Nat. Clim. Change* **11** 319–25

Kumar S and Khanna M 2019 Temperature and production efficiency growth: empirical evidence *Clim. Change* **156** 209–29

Marsh T, Kirby C, Muchan K, Barker L, Henderson E and Hannaford J 2016 *The Winter Floods of 2015/2016 in the UK—A Review* Centre for Ecology & Hydrology 978-1-906698-61-4

Metcalf G E and Stock J H 2017 Integrated assessment models and the social cost of carbon: a review and assessment of U.S. experience *Rev. Environ. Econ. Policy* **11** 80–99

Moore F C and Diaz D B 2015 Temperature impacts on economic growth warrant stringent mitigation policy *Nat. Clim. Change* **5** 127–31

Moore F C, Rising J, Lollo N, Springer C, Vasquez V, Dolginow A, Hope C and Anthoff D 2018 Mimi-PAGE, an open-source implementation of the PAGE09 integrated assessment model *Sci. Data* **5** 180187

Morice C P, Kennedy J J, Rayner N A and Jones P D 2012 Quantifying uncertainties in global and regional temperature change using an ensemble of observational estimates: the HadCRUT4 data set *J. Geophys. Res.: Atmos.* **117** D08101

Moyer E J, Woolley M D, Matteson N J, Glotter M J and Weisbach D A 2014 Climate impacts on economic growth as drivers of uncertainty in the social cost of carbon *J. Leg. Stud.* **43** 401–25

National Academies of Sciences Engineering and Medicine 2017 *Valuing Climate Damages: Updating Estimation of the Social Cost of Carbon Dioxide* First (Washington, DC: National Academies Press) p 280

Nordhaus W D 2017 Revisiting the social cost of carbon *Proc. Natl Acad. Sci. USA* **114** 1518–23

O'Neill B C *et al* 2016 The Scenario Model Intercomparison Project (ScenarioMIP) for CMIP6 *Geosci. Model Dev.* **9** 3461–82

Otto A, Todd B J, Bowerman N, Frame D J and Allen M R 2013 Climate system properties determining the social cost of carbon *Environ. Res. Lett.* **8** 024032

Otto C, Piontek F, Kalkuhl M and Frieler K 2020 Event-based models to understand the scale of the impact of extremes *Nat. Energy* **5** 111–14

Pindyck R S 2013 Climate change policy: what do the models tell us? *J. Econ. Lit.* **51** 860–72

Pindyck R S 2019 The social cost of carbon revisited *J. Environ. Econ. Manage.* **94** 140–60

Piontek F *et al* 2021 Integrated perspective on translating biophysical to economic impacts of climate change *Nat. Clim. Change* **11** 563–72

Piontek F, Kalkuhl M, Kriegler E, Schultes A, Leimbach M, Edenhofer O and Bauer N 2019 Economic growth effects of alternative climate change impact channels in economic modeling *Environ. Resour. Econ.* **73** 1357–85

Ricke K, Drouet L, Caldeira K and Tavoni M 2018 Country-level social cost of carbon *Nat. Clim. Change* **8** 895–900

Rising J, Waidelich P and Kikstra J S 2021 *PAGE-2020 with growth effects and interannual temperature variability* (https://zenodo.org/record/3907851)

Rogelj J *et al* 2018 Scenarios towards limiting global mean temperature increase below 1.5 °C *Nat. Clim. Change* **8** 325–32

Rose S K, Diaz D B and Blanford G J 2017 Understanding the social cost of carbon: a model diagnostic and inter-comparison study *Clim. Change Econ.* **08** 1750009

Seneviratne S *et al* 2012 Changes in climate extremes and their impacts on the natural physical environment *Technical Report*

Shine K P, Derwent R, Wuebbles D J and Morcrette J 1990 Radiative forcing of climate *Technical Report*

Sippel S, Zscheischler J, Heimann M, Otto F E L, Peters J and Mahecha M D 2015 Quantifying changes in climate variability and extremes: Pitfalls and their overcoming *Geophys. Res. Lett.* **42** 9990–8

Smith L A and Stern N 2011 Uncertainty in science and its role in climate policy *Phil. Trans. R. Soc.* A **369** 4818–41

Stern N H 2007 *The Economics of Climate Change: The Stern Review* (Cambridge: Cambridge University Press)

Stern N and Stiglitz J 2021 The social cost of carbon, risk, distribution, market failures: an alternative approach *Technical Report* (Cambridge, MA: National Bureau of Economic Research)

Stiglitz J E *et al* 2017 Report of the high-level commission on carbon prices *Technical Report* (Washington, DC)

Stocker T et al 2013 *Climate Change 2013: The Physical Science Basis. Contribution of Working Group I to the Fifth Assessment Report of the Intergovernmental Panel on Climate Change* (*Technical Summary*) (Cambridge: Cambridge University Press)

Tol R S 2018 The economic impacts of climate change *Rev. Environ. Econ. Policy* **12** 4–25

Tol R S 2019 A social cost of carbon for (almost) every country *Energy Econ.* **83** 555–66

Umwelt Bundesamt 2019 *Gesellschaftliche Kosten von Umweltbelastungen* (available at: www.umweltbundesamt.de/daten/umwelt-wirtschaft/gesellschaftliche-kosten-von-umweltbelastungen#gesamtwirtschaftliche-bedeutung-der-umweltkosten)

Van Vuuren D P, Van der Wijst K-I, Marsman S, Van den Berg M, Hof A F and Jones C D 2020 The costs of achieving climate targets and the sources of uncertainty *Nat. Clim. Change* **10** 329–34

Wagner G, Anthoff D, Cropper M, Dietz S, Gillingham K T, Groom B, Kelleher P, Moore F C and Stock J H 2021 Eight priorities for calculating the social cost of carbon *Nature* **590** 548–50

Weitzman M 2014 Fat tails and the social cost of carbon: a super-simple expository model of the SCC *J. Econ. Lit.* **104** 1–7

Yumashev D *et al* 2019 Climate policy implications of nonlinear decline of arctic land permafrost and other cryosphere elements *Nat. Commun.* **10** 1900